Panel-Point Model for Rigidity and Flexibility Analysis of Rigid Origami

Kentaro Hayakawa[a,*], Zeyuan He[b], Simon D. Guest[b]

[a] *Department of Architecture and Architectural Engineering, Kyoto University, Kyoto-Daigaku Katsura, Nishikyo, Kyoto, 615-8540, , Japan*
[b] *Department of Engineering, University of Cambridge, Civil Engineering Building, 7a JJ Thomson Ave, Cambridge, CB3 0FA, , United Kingdom*

Abstract

In this study, we lay the groundwork for a systematic investigation of the rigidity and flexibility of rigid origami by using the mathematical model referred to as the panel-point model. Rigid origami is commonly known as a type of panel-hinge structure where rigid polygonal panels are connected by rotational hinges, and its motion and stability are often investigated from the perspective of its consistency constraints representing the rigidity and connection conditions of panels. In the proposed methodology, vertex coordinates are directly treated as the variables to represent the rigid origami in the panel-point model, and these variables are constrained by the conditions for the out-of-plane and in-plane rigidity of panels. This model offers several advantages including: 1) the simplicity of polynomial consistency constraints; 2) the ease of incorporating displacement boundary conditions;

*Corresponding author
Email addresses: `se.hayakawa@archi.kyoto-u.ac.jp` (Kentaro Hayakawa), `zh299@cam.ac.uk` (Zeyuan He), `sdg@eng.cam.ac.uk` (Simon D. Guest)

and 3) the straightforwardness of numerical simulation and visualization. It is anticipated that the presented theories in this article are valuable to a broad audience, including mathematicians, engineers, and architects.
Keywords: Rigid origami, statics, rigidity, stability, prestress

---

1. Introduction

1.1. Background

This paper presents a methodology for the analysis of the rigidity and flexibility of rigid origami using a *panel-point model*. *Rigid origami* is a kind of panel-hinge structure where rigid polygonal panels are connected by rotational hinges referred to as the *crease lines*. In the panel-point model, a rigid origami is described by its vertex positions, rather than the folding angles, used in a previous related study [1]. It offers simple and systematic formulations of consistency constraints and their derivatives.

Origami offers new topics and solutions to a wide range of fields in mathematics [2, 3] and engineering [4, 5], and has been actively studied in recent years. In particular, rigid origami is subject to the strict requirement of folding without deformation of its faces, and the properties of rigid origami's folding mechanisms are the subject of study in mathematics, physics and engineering.

From a theoretical perspective, rigid origami is sometimes associated with rigidity theory, and sometimes with the kinematics and mechanics that describe its motion. In kinematics and mechanics, the motion of a rigid origami is investigated with respect to consistency constraints on the variables describing a motion or a displacement of a rigid origami. To formulate the consistency constraints, a rigid origami is often modelled as a structure consisting of hinge-connected rigid panels or an equivalent linkage, and the variables are selected to represent the (relative) displacements or positions of the components of the rigid origami model; e.g., folding angles [6], or displacements, or coordinates of nodes [7, 8, 9, 10]. The construction of a model or a mathematical representation of a rigid origami is a crucial step because it greatly affects the simplicity of the resultant symbolic and numerical calculations, mechanism analysis, and folding simulation.

The rigidity of rigid origami, which is the focus of this study, was recently introduced by He and Guest [1] using a folding angle formulation. Here we revisit this rigidity analysis, but using a panel-point model, which has a number of advantages. In contrast to the motion analysis of a rigid origami, which has been widely studied, rigidity theory investigates the conditions where a rigid origami is *not* foldable. The rigidity concepts employed in this study are similar to those of the structural rigidity theory for classical bar-joint frameworks [11, 12, 13]. In the original study [1], several levels of rigidity are discussed in accordance with the classical structural rigidity theory; first-order rigidity, static rigidity, prestress stability, and second-order rigidity. These rigidity concepts are also investigated for the panel-point model in this study by invoking the ideas used in the field of combinatorial rigidity [14, 15]. While the treatment of the equations follows that in classical rigidity theory,

Table 1: Classification of models of rigid origami with respect to the choice of the variables and the analysis type: Classification of the analysis is based on Ref. [16].

Analysis type	Choice of variables	
	Vertex position description	Folding angle description
Kinematic-based; rigid faces and crease lines without rotational stiffness	**Panel-point model**	Rotational hinge model [1, 6, 17, 18]
Intermediate; analysis with mixed conditions in two types of analysis	Rigid truss model [7] Truss model with pyramid framework [8] Frame model [9, 10]	
Mechanics-based; elastic (plastic) faces and crease lines	Bar and hinge model [19, 20] Finite element model with shell elements [20, 21]	

this study contributes to the field by presenting a new construction and physical interpretation of a rigid origami model, which will also be useful to allow origami engineers to systematically develop a mechanism analysis using the proposed model.

1.2. Analysis and models of rigid origami

This section provides a comprehensive review of the characteristics of various models of rigid origami, and the advantages of the panel-point model are summarized. Models and mathematical representations of rigid origami can be classified with respect to their variables and the analysis types where they are used (see Table 1 and Fig. 1). The variables can be roughly classified into a *vertex position description* (nodal position description) or a *folding angle description*. The former uses the positions of the vertices or other specified parts of a rigid origami as variables. Therefore, it can directly

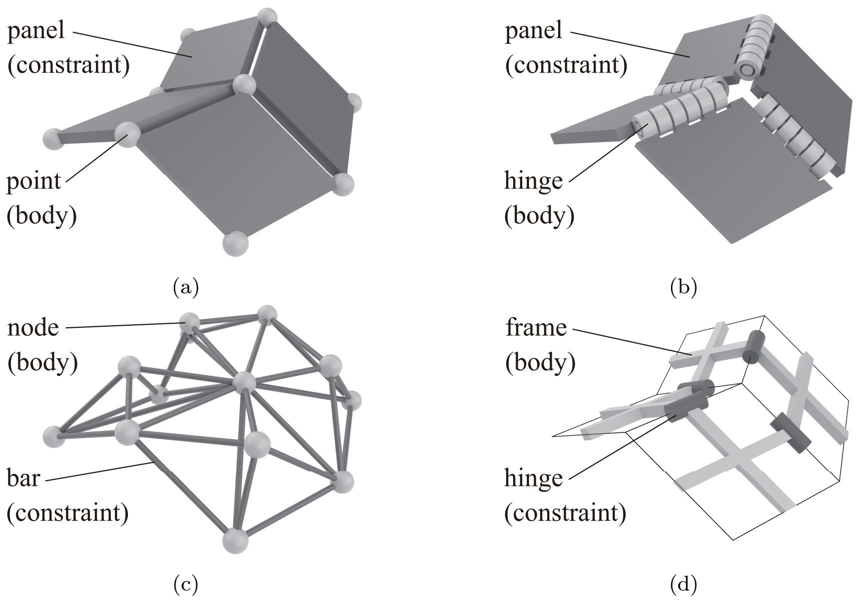

Figure 1: Models of rigid origami where the physical representation of the bodies for expressing the deformation of rigid origami are indicated by grey components and the physical representation of the constraints are indicated by black components; (a) Panel-point model consisting of points constrained by panels. (b) Rotational hinge model consisting of hinges constrained by panels. (c) Truss model consisting of nodes constrained by bars. (d) Frame model consisting of frames constrained by hinges.

represent the shape of an origami in three-dimensional space, and it is easy to introduce displacement boundary conditions and visualize the shape. The latter takes the folding angles of the crease lines (the complementary angles of the pairs of faces adjacent to the crease lines) as variables. Although the folding angle description is the simplest way to express the folding state, it is not easy to introduce boundary conditions because of the complicated nonlinear relationship of the vertex positions to the folding angles.

Depending on the level of idealization of the structure, the analysis of rigid origami can be classified into three major types: kinematic-based analysis, mechanics-based analysis, and intermediate analysis. Kinematic-based analysis assumes that each face is not deformed, and only the relative rotation of the faces at each crease line occurs as the deformation of an origami. Mechanics-based analysis considers elastic or plastic deformation of the faces under external loads or forced displacements, and often considers rotational stiffness of the crease lines; i.e., the physical properties of the materials and elements are incorporated. As an intermediate between the above two types, the analysis is also often performed to find an equilibrium state with external loads as considered in the mechanics-based analysis under the assumption of the rigid faces in the kinematic-based analysis. Further details on the various analyses and models can be found in Ref. [16].

As shown in Table 1, the panel-point model is introduced for performing kinematic-based analysis in the vertex position description, which has not been covered so far. The vertex positions are explicitly treated as the variables, and these variables are constrained by the consistency constraints to guarantee the rigidity of panels. The consistency constraint equations are formulated in polynomial form with respect to the in-plane and out-of-plane deformation of each panel which correspond to *length constraints* and *coplanar constraints*, respectively. Here, for each panel, the *in-plane* direction is parallel to the plane in which the panel is located, and the *out-of-plane* direction is orthogonal to it. The former constraints are formulated to constrain the length of all boundary edges of a face and some diagonals when the face has more than three edges. The latter constraints are formulated so that for each constraint, four of the vertices of a face are on the same plane, and for a face with more than four edges, several coplanar constraints are imposed. The choice of vertex sets for the imposition of length and coplanar constraints is generically arbitrary, and it is shown that the choice does not affect the rigidity and flexibility considered in this paper although the distribution of internal forces corresponding to the constraints may change. Note that the length constraints are equivalent to the formulation used in the truss model or the bar-joint structures, while the coplanar constraints differ: the coplanar constraints in the truss model are usually formulated as trigonometric equations, or small out-of-plane deformation is penalized by applying a high bending stiffness to the panels in the intermediate or the mechanics-based analysis.

As a final comparison between the models used for the kinematic-based analysis in Table 1, Table 2 juxtaposes features of the point-panel model with the rotational hinge model [1]. The notable advantages of the model used in this study are:

1. the simplicity of consistency constraints, which are in polynomial form,
2. the ease of incorporating displacement boundary conditions,
3. the straightforwardness of numerical simulation and visualization,
4. the intuitively comprehensible physical interpretation of loads and internal forces.

1.3. Structure of this article

Section 2 presents the formulation of the length and coplanar constraints based on the structure of the underlying graph of a rigid origami. In Sections 3 – 6, rigidity analysis of a rigid origami is presented following the definitions of rigidity and flexibility in Ref. [1]. First-order rigidity and flex are defined in Section 3 using first-order derivatives of the constraints. Sections 4 and 5 introduce the idea of load and internal force in the context of rigidity analysis and discuss the static rigidity and prestress stability of the point-panel model. In addition, section 6 discusses second-order rigidity as the next level of rigidity. Although some studies have discussed higher-order flexibility in the bar-joint framework [22, 23], the present paper only considers this up to second-order. Note that the displacement boundary conditions are not considered in Sections 3 – 6 for simplicity, but are introduced in Section 7. Finally, the conclusions of this paper are provided in Section 8.

Table 2: Comparison between a panel-point model (vertex position description) and a rotational hinge model (folding angle description) in several aspects of symbolical analysis and simulation.

	Panel-point model	Rotational hinge model
Applicability	any surfaces	only for orientable surfaces
Forms of consistency constraints	length and coplanar constraints in polynomial form	loop conditions in trigonometric equations
Compatibility with boundary condition	convenient for any form of displacement boundary conditions both symbolically and numerically	impractical for analysis with displacement boundary conditions
Compatibility with external loads	straightforward for point loads	straightforward for moments applied to a crease line
Utility in flexibility and stability analysis	convenient for symbolic analysis on local rigidity, generic rigidity, and stability	convenient for symbolic analysis on local rigidity, generic rigidity, and stability
Utility in folding simulation	convenient for numerical simulation by integration over a field of first-order flex	convenient for numerical simulation by integration over a field of first-order flex
Utility in visualization and construction	convenient for visualization due to the explicit representation of vertex position in Euclidean space	need to transfer the folding angles to Euclidean coordinates using the dimension of faces

2. Modelling

Here, the modelling of the point-panel model is introduced. An example of a realization is shown in Fig. 2(a).

Definition 2.1. A hypergraph G is a finite nonempty set of objects called *vertices* together with a (possibly empty) set of subsets of distinct vertices of G called *hyper edges*.

The *underlying graph* G for a rigid origami is a hypergraph with a cyclic order (either forward or backward) of each hyper edge, called a *cyclic hyper edge*. The vertices in a cyclic hyper edge form a panel in a cyclic sequence.

A *realization* $\boldsymbol{p}$ of an underlying graph G (or written as $G(\boldsymbol{p})$) is a rigid origami where n^{v} vertex position vectors $p_1, p_2, \ldots, p_{n^{\mathrm{v}}} \in \mathbb{R}^3$ are assembled into a column vector $\boldsymbol{p} \in \mathbb{R}^{3n^{\mathrm{v}}}$ (suppose the number of vertices is n^{v}). In this study, the following notation is used to denote a vector of vectors for convenience:

$$\boldsymbol{p} = (p_1;\, p_2;\, \ldots;\, p_{n^{\mathrm{v}}}) = \begin{pmatrix} p_1 \\ p_2 \\ \vdots \\ p_{n^{\mathrm{v}}} \end{pmatrix}.$$

We use a 'hyper edge' not to represent a panel but to refer to a sequence of vertices that can form a panel, including the case where these vertices are placed in an unfavourable way, such as a non-coplanar arrangement. For example, the hypergraph shown in Fig. 2(a) has 8 cyclic hyper edges, each

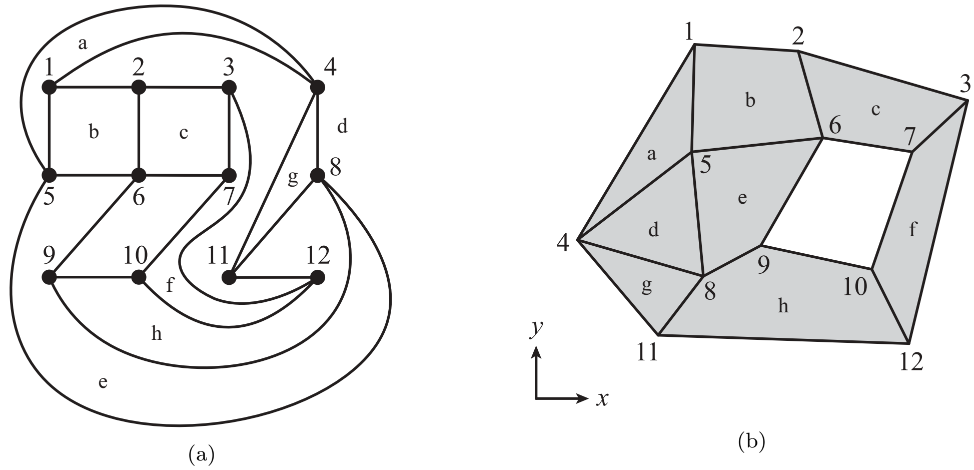

Figure 2: (a) An underlying graph of a rigid origami in the point-panel model, which has 8 cyclic hyper edges a–h. (b) A planar realization of (a), where the lower-case roman labels indicate the correspondence between the hyper edges of (a) and the panels of (b).

of which forms a panel in the cyclic order:

$$\{1,\ 4,\ 5\},\ \{1,\ 5,\ 6,\ 2\},\ \{2,\ 6,\ 7,\ 3\},\ \{4,\ 8,\ 5\},$$
$$\{5,\ 8,\ 9,\ 6\},\ \{3,\ 7,\ 10,\ 12\},\ \{4,\ 11,\ 8\},\ \{8,\ 11,\ 12,\ 10,\ 9\}.$$

A realization $\boldsymbol{p}$ needs to satisfy *coplanar constraints* and *length constraints* to guarantee the planarity of the panel and to fix the dimension of the panel, respectively. We investigate the rigidity of rigid origami for any realization $\boldsymbol{p}$ satisfying the given coplanar and length constraints except for some special cases where the coplanarity or the dimension of a panel may not be guaranteed. In other words, the coplanar and length constraints are assigned before the realization $\boldsymbol{p}$ is determined. These constraints are imposed on the vertices on each cyclic hyper edge in two ways referred to as: 1) *elementary*

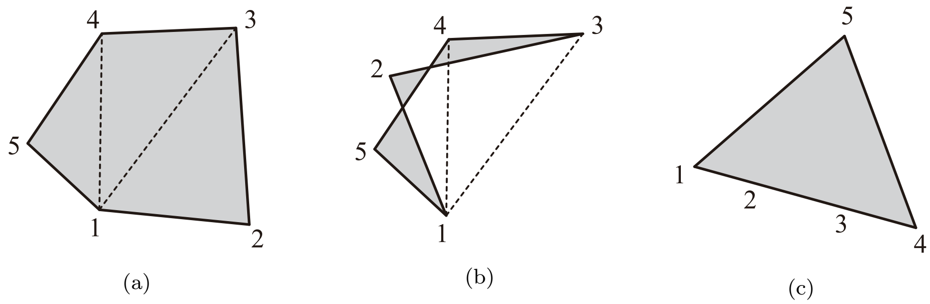

Figure 3: Realizations of a five sided panel under 2 elementary coplanar constraints and 7 elementary length constraints fixing 5 boundary lines and 2 diagonals connecting vertices 1 and 3, and vertices 1 and 4; (a), (b) Two different generic realizations obtained under the same set of d_{ij} for the elementary length constraints. (c) A non-generic realization with colinear vertices 1 – 4 where the elementary coplanar constraints are not enough to ensure coplanarity of the panel.

constraints and 2) *elementary + additional* constraints

(1) Elementary coplanar and length constraints

The elementary coplanar constraints are imposed on $m-3$ sets of four of m vertices on each cyclic hyper edge with m sides. For example, the model in Fig. 2, with 8 cyclic hyper edges, has 6 coplanar constraints. The coplanar constraints are represented as cubic polynomial equations, as described below, that ensure that the vertices on each cyclic hyper edge are coplanar. For a single hyper edge with m vertices, $m-3$ elementary coplanar constraints are assigned so that at least three vertices in any single coplanar constraint are shared with at least one other coplanar constraint, and the constraint over $p_i,\ p_j,\ p_k,\ p_l$ is written as:

$$\begin{gathered} f^{\mathrm{c}}(i,\, j,\, k,\, l) = \langle (p_j - p_i) \times (p_k - p_i),\, p_l - p_i \rangle = 0 \\ \text{for all selected } i,\, j,\, k,\, l \in \mathbb{Z}^+, i,\, j,\, k,\, l \leq n^{\mathrm{v}}, \end{gathered} \tag{1}$$

where the symbol $\langle \cdot,\, \cdot \rangle$ stands for a inner product of vectors. f^{c} in the above equation is the signed volume of the parallelepiped formed by $p_j - p_i$, $p_k - p_i$ and $p_l - p_i$. Although the order of four vertices in Eq. (1) is not crucial, we assume that vertices $i,\, j,\, k,\, l$ are arranged in this order in a cyclic hyper edge. Then, the coplanar constraints f^{c} for all hyper edges are assembled into an n^{c} column vector $\boldsymbol{f}^{\mathrm{c}} \in \mathbb{R}^{n^{\mathrm{c}}}$, where n^{c} is the total number of coplanar constraints for the entire rigid origami. Note that the coplanarity of the vertices may not be guaranteed by the elementary coplanar constraints for a realization where some vertices are colinear, as for the example shown in Fig. 3(c), but such pathological cases are excluded from the discussion here.

Elementary length constraints are assigned to fix the lengths of all boundary lines and $m - 3$ diagonals of each panel with m sides. The $m - 3$ length constraints on diagonals should be chosen in a way such that any p ($p \in \mathbb{Z}^+,\ 2 \leq p \leq m - 1$) vertices of this panel have $2p - 3$ of these length constraints. Each of these constraints is a quadratic polynomial equation over $\boldsymbol{p}$ with the form:

$$\begin{gathered} f^{\mathrm{l}}(i,\, j) = \frac{1}{2} \left(\langle p_i - p_j,\, p_i - p_j \rangle - d_{ij}^2 \right) = 0 \\ \text{for all selected } i,\ j \in \mathbb{Z}^+,\ i < j \leq n^{\mathrm{v}}. \end{gathered} \tag{2}$$

$d_{ij} \in \mathbb{R}$ is the distance between p_i and p_j which is positive and satisfy the triangle inequality. The collection of elementary length constraints f^{l} for the entire rigid origami is written by an n^{l} column vector $\boldsymbol{f}^{\mathrm{l}} \in \mathbb{R}^{n^{\mathrm{l}}}$, where n^{l} is the total number of elementary length constraints for the entire rigid origami. Note that the shape of a panel with more than three sides cannot be uniquely determined in a realization $\boldsymbol{p}$ under the elementary coplanar and length constraints as shown in Figs. 3(a) and 3(b), both of which have the same constraints.

(2) Elementary + additional coplanar and length constraints

We can also impose coplanar and length constraints on all possible sets of vertices on each cyclic hyper edge. Constraints added to elementary coplanar and length constraints are referred to as the additional coplanar constraints and the additional length constraints, respectively. The number of the additional coplanar constraints on each m-sided panel is $\binom{m}{4} - m + 3$, and the number of the additional length constraints is $(m-2)(m-3)/2$. These additional coplanar and length constraints are written by an n^{ca} column vector $\boldsymbol{f}^{\mathrm{ca}} \in \mathbb{R}^{n^{\mathrm{ca}}}$ and an n^{la} column vector $\boldsymbol{f}^{\mathrm{la}} \in \mathbb{R}^{n^{\mathrm{la}}}$, respectively, where n^{ca} and n^{la} are the total numbers of additional coplanar and length constraints for the entire rigid origami, respectively. When the additional coplanar and length constraints are assigned in addition to the elementary coplanar and length constraints, the shape of each panel is uniquely determined in a realization $\boldsymbol{p}$ although there are many redundant constraints with respect to the rigidity of rigid origami. The redundancy is reflected in the rank of the rigidity matrix defined below.

Definition 2.2. (1) Let $\boldsymbol{f} = (\boldsymbol{f}^{\mathrm{c}};\ \boldsymbol{f}^{\mathrm{l}};\ \boldsymbol{f}^{\mathrm{ca}};\ \boldsymbol{f}^{\mathrm{la}})$. The solution space $\mathcal{P}$ of realizations $\boldsymbol{p}$ is defined as:

$$\mathcal{P} = \{\boldsymbol{p} \in \mathbb{R}^{3n^{\mathrm{v}}} \mid \boldsymbol{f}(\boldsymbol{p}) = \boldsymbol{0} \\ \text{for } \textbf{a given set} \text{ of } d_{ij} \text{ in the length constraints}\},$$

where d_{ij} are the distances which are included in $n^{\mathrm{l}} + n^{\mathrm{la}}$ length constraints and are subject to the triangle inequality.

The extended solution space $\widetilde{\mathcal{P}}$ is also defined as:

$$\widetilde{\mathcal{P}} = \{\boldsymbol{p} \in \mathbb{R}^{3n^{\mathrm{v}}} \mid \boldsymbol{f}(\boldsymbol{p}) = \boldsymbol{0} \\ \text{for } \textbf{all admissible } d_{ij} \text{ in the length constraints}\}.$$

Here, ‘admissible’ d_{ij} are any possible distances subject to the triangle inequality.

(2) The *rigidity matrix* of the entire rigid origami is the Jacobian of $\boldsymbol{f}$:

$$\frac{\mathrm{d}\boldsymbol{f}}{\mathrm{d}\boldsymbol{p}} = \frac{\mathrm{d}(\boldsymbol{f}^{\mathrm{c}};\ \boldsymbol{f}^{\mathrm{l}};\ \boldsymbol{f}^{\mathrm{ca}};\ \boldsymbol{f}^{\mathrm{la}})}{\mathrm{d}\boldsymbol{p}},$$

which is the $(n^{\mathrm{c}} + n^{\mathrm{l}} + n^{\mathrm{ca}} + n^{\mathrm{la}}) \times 3n^{\mathrm{v}}$ matrix whose (i, j) component is the first-order partial derivative of the i-th component of $\boldsymbol{f}$ with respect to the j-th component of $\boldsymbol{p}$ $(i,\ j \in \mathbb{Z}^{+},\ i \le n^{\mathrm{c}} + n^{\mathrm{l}} + n^{\mathrm{ca}} + n^{\mathrm{la}},\ j \le 3n^{\mathrm{v}})$. Note that $\mathrm{d}\boldsymbol{f}/\,\mathrm{d}\boldsymbol{p}$ is independent of any d_{ij}.

(3) $\boldsymbol{p} \in \mathcal{P}$ is a *panel-wise generic* realization if the determinant of a submatrix of $\mathrm{d}\boldsymbol{f}/\,\mathrm{d}\boldsymbol{p}$ consisting of the rows and columns corresponding to the constraints and the vertices of each cyclic hyper edge (i.e., a rigidity matrix of each panel) is zero only if for any $\boldsymbol{q} \in \widetilde{\mathcal{P}}$, the determinant of the corresponding submatrix of $\mathrm{d}\boldsymbol{f}/\,\mathrm{d}\boldsymbol{q}$ is zero.

Note that the displacement boundary conditions are not considered in the construction of the theories in Sections 3 – 6 for simplicity. The instructions for the formulation of the additional constraints representing the displacement boundary conditions and the extension of the idea of rigidity under the boundary conditions are given in Section 7.

Proposition 2.3 below is a quick note on the invariance of the rank of the rigidity matrix with respect to choices of vertices in the coplanar constraints and diagonals in the length constraints.

Proposition 2.3. (Invariance of the rank of rigidity matrix) Different choices of coplanar and length constraints have no effect on the rank of the rigidity matrix at a panel-wise generic realization:

(1) Additional constraints forming $\boldsymbol{f}^{\mathrm{ca}}$ and $\boldsymbol{f}^{\mathrm{la}}$ do not change the rank of the rigidity matrix:

$$\operatorname{rank}\left(\frac{\mathrm{d}(\boldsymbol{f}^{\mathrm{c}};\ \boldsymbol{f}^{\mathrm{l}})}{\mathrm{d}\boldsymbol{p}}\right) = \operatorname{rank}\left(\frac{\mathrm{d}\boldsymbol{f}}{\mathrm{d}\boldsymbol{p}}\right).$$

(2) Different choices of vertices for elementary coplanar constraints do not change the rank of the rigidity matrix. In order words, suppose there are

two choices of coplanar constraints $\boldsymbol{f}^{\mathrm{c}_1}$ and $\boldsymbol{f}^{\mathrm{c}_2}$:

$$\operatorname{rank}\left(\frac{\mathrm{d}(\boldsymbol{f}^{\mathrm{c}_1};\ \boldsymbol{f}^{\mathrm{l}})}{\mathrm{d}\boldsymbol{p}}\right) = \operatorname{rank}\left(\frac{\mathrm{d}(\boldsymbol{f}^{\mathrm{c}_2};\ \boldsymbol{f}^{\mathrm{l}})}{\mathrm{d}\boldsymbol{p}}\right).$$

(3) Different choices of diagonals for elementary length constraints do not change the rank of the rigidity matrix. In other words, suppose there are two choices of diagonals $\boldsymbol{f}^{\mathrm{l}_1}$ and $\boldsymbol{f}^{\mathrm{l}_2}$:

$$\operatorname{rank}\left(\frac{\mathrm{d}(\boldsymbol{f}^{\mathrm{c}};\ \boldsymbol{f}^{\mathrm{l}_1})}{\mathrm{d}\boldsymbol{p}}\right) = \operatorname{rank}\left(\frac{\mathrm{d}(\boldsymbol{f}^{\mathrm{c}};\ \boldsymbol{f}^{\mathrm{l}_2})}{\mathrm{d}\boldsymbol{p}}\right).$$

Proof. The proof is included in the proof of Proposition 3.3. □

Example 1. Consider the example shown in Fig. 2(b) with 20 boundary lines of panels and 12 vertices. The number of elementary coplanar, elementary length, additional coplanar, and additional length constraints are $n^{\mathrm{c}} = 6$, $n^{\mathrm{l}} = 26$, $n^{\mathrm{ca}} = 3$, and $n^{\mathrm{la}} = 7$, respectively. The size of $\boldsymbol{p}$ is $3n^{\mathrm{v}} = 36$. Hence, $\mathrm{d}\boldsymbol{f}/\,\mathrm{d}\boldsymbol{p}$ is a 39×36 matrix. At the planar realization shown in Fig. 2(b), $\operatorname{rank}(\mathrm{d}\boldsymbol{f}/\,\mathrm{d}\boldsymbol{p}) = 27$, while at 'most' non-planar panel-wise generic realizations, $\operatorname{rank}(\mathrm{d}\boldsymbol{f}/\,\mathrm{d}\boldsymbol{p}) = 30$.

3. Rigidity matrix and first-order rigidity

For a coplanar constraint over four vertices $p_i,\ p_j,\ p_k,\ p_l$ on the same hyper edge, non-zero submatrices of the rigidity matrix are calculated from

Eq. (1) as:

$$\begin{aligned}
\frac{\partial f^{\mathrm{c}}(i,\, j,\, k,\, l)}{\partial p_i} &= \{(p_j - p_k) \times (p_l - p_k)\}^{\mathsf{T}}, \\
\frac{\partial f^{\mathrm{c}}(i,\, j,\, k,\, l)}{\partial p_j} &= -\{(p_k - p_l) \times (p_i - p_l)\}^{\mathsf{T}}, \\
\frac{\partial f^{\mathrm{c}}(i,\, j,\, k,\, l)}{\partial p_k} &= \{(p_l - p_i) \times (p_j - p_i)\}^{\mathsf{T}}, \\
\frac{\partial f^{\mathrm{c}}(i,\, j,\, k,\, l)}{\partial p_l} &= -\{(p_i - p_j) \times (p_k - p_j)\}^{\mathsf{T}}, \\
&\text{for selected } i,\, j,\, k,\, l \in \mathbb{Z}^+, i,\, j,\, k,\, l \le n^{\mathrm{v}}.
\end{aligned} \tag{3}$$

Also, for a length constraint written as Eq. (2):

$$\begin{aligned}
\frac{\partial f^{\mathrm{l}}(i,\, j)}{\partial p_i} &= (p_i - p_j)^{\mathsf{T}}, \\
\frac{\partial f^{\mathrm{l}}(i,\, j)}{\partial p_j} &= (p_j - p_i)^{\mathsf{T}}, \\
&\text{for selected } i,\ j \in \mathbb{Z}^+,\ i < j \le n^{\mathrm{v}}.
\end{aligned} \tag{4}$$

An entire rigidity matrix $\mathrm{d}\boldsymbol{f}/\mathrm{d}\boldsymbol{p}$ is obtained by assembling the derivatives of constraints. For example, two rows of the rigidity matrix of the rigid origami in Fig. 2, whose vertex coordinates are not fixed, are shown below:

$$\begin{aligned}
\frac{\partial f^{\mathrm{c}}(1,\, 2,\, 6,\, 5)}{\partial \boldsymbol{p}} = \Big[& \ \{(p_2 - p_6) \times (p_5 - p_6)\}^{\mathsf{T}} \quad -\{(p_6 - p_5) \times (p_1 - p_5)\}^{\mathsf{T}} \quad 0 \quad 0 \\
& -\{(p_1 - p_2) \times (p_6 - p_2)\}^{\mathsf{T}} \quad \{(p_5 - p_1) \times (p_2 - p_1)\}^{\mathsf{T}} \quad 0 \quad 0 \quad 0 \quad 0 \quad 0 \quad 0 \ \Big],
\end{aligned}$$

$$\frac{\partial f^{\mathrm{l}}(1,\, 2)}{\partial \boldsymbol{p}} = \begin{bmatrix} (p_1 - p_2)^{\mathsf{T}} & (p_2 - p_1)^{\mathsf{T}} & 0 & 0 & 0 & 0 & 0 & 0 & 0 & 0 & 0 & 0 \end{bmatrix}.$$

Every 0 in the above equations is a 1×3 zero row vector in the above matrix form.

Definition 3.1. Suppose the rank of the rigidity matrix is:

$$\operatorname{rank}\left(\frac{\mathrm{d}\boldsymbol{f}}{\mathrm{d}\boldsymbol{p}}\right) = q \ (q \in \mathbb{Z}^+,\ q \leq \min(n^{\mathrm{c}} + n^{\mathrm{l}},\ 3n^{\mathrm{v}} - 6))$$

at a realization $\boldsymbol{p} \in \mathcal{P}$. Here, n^{v}, n^{c}, and n^{l} are the number of vertices, elementary coplanar constraints, and elementary length constraints, respectively.

A rigid origami $G(\boldsymbol{p})$ is *first-order rigid* if $q = 3n^{\mathrm{v}} - 6$.

A *first-order flex* $\boldsymbol{p}' = (p'_1;\ p'_2;\ \ldots;\ p'_{n^{\mathrm{v}}}) \in \mathbb{R}^{3n^{\mathrm{v}}}$ is a vector in the nullspace of $\mathrm{d}\boldsymbol{f}/\,\mathrm{d}\boldsymbol{p}$ whose dimension is $3n^{\mathrm{v}} - q$; i.e, $\boldsymbol{p}'$ satisfies:

$$\frac{\mathrm{d}\boldsymbol{f}}{\mathrm{d}\boldsymbol{p}}\boldsymbol{p}' = \boldsymbol{0}. \tag{5}$$

A *trivial first-order flex* is:

$$p'_i = Ap_i + u,\ i \in \mathbb{Z}^+,\ i \leq n^{\mathrm{v}}, \tag{6}$$

where $A \in \mathbb{R}^{3\times 3}$ and $u \in \mathbb{R}^3$ are a fixed skew-symmetric matrix and a fixed translation vector common to all vertices, respectively. The dimension of space of trivial first-order flex is 6 without displacement boundary conditions.

Remark 3.2. The panel-wise genericity of a realization $\boldsymbol{p}$ in Definition 2.2 implies the first-order rigidity of each panel.

Proposition 3.3 below and the several following propositions show the invariance in the first-order and second-order analyses. This invariance indicates that, as long as the realization is panel-wise generic, the proposed panel-point model is robust to the choices of coplanar and length constraints that may be differently set by users of the model.

Proposition 3.3. (Invariance of first-order flex) Different choices of coplanar and length constraints have no effect on the space of first-order flex at a panel-wise generic realization:

(1) Additional coplanar and length constraints do not change the space of first-order flex. In other words, $\mathrm{d}\boldsymbol{f}/\,\mathrm{d}\boldsymbol{p}$ and $\mathrm{d}(\boldsymbol{f}^{\mathrm{c}};\, \boldsymbol{f}^{\mathrm{l}})/\,\mathrm{d}\boldsymbol{p}$ have the same nullspace:

$$\frac{\mathrm{d}(\boldsymbol{f}^{\mathrm{c}};\, \boldsymbol{f}^{\mathrm{l}})}{\mathrm{d}\boldsymbol{p}}\boldsymbol{p}' = \mathbf{0} \Leftrightarrow \frac{\mathrm{d}\boldsymbol{f}}{\mathrm{d}\boldsymbol{p}}\boldsymbol{p}' = \mathbf{0}.$$

(2) Different choices of vertices for elementary coplanar constraints do not change the space of first-order flex. In order words, suppose there are two choices of coplanar constraints $\boldsymbol{f}^{\mathrm{c}_1}$ and $\boldsymbol{f}^{\mathrm{c}_2}$, they satisfy the following relation:

$$\frac{\mathrm{d}(\boldsymbol{f}^{\mathrm{c}_1};\, \boldsymbol{f}^{\mathrm{l}})}{\mathrm{d}\boldsymbol{p}}\boldsymbol{p}' = \mathbf{0} \Leftrightarrow \frac{\mathrm{d}(\boldsymbol{f}^{\mathrm{c}_2};\, \boldsymbol{f}^{\mathrm{l}})}{\mathrm{d}\boldsymbol{p}}\boldsymbol{p}' = \mathbf{0}.$$

(3) Different choice of diagonals for elementary length constraints do not change the space of first-order flex. In other words, suppose there are two choices of diagonals to form the elementary length constraints $\boldsymbol{f}^{\mathrm{l}_1}$

and $\boldsymbol{f}^{\mathrm{l}_2}$, they satisfy the following relation:

$$\frac{\mathrm{d}(\boldsymbol{f}^{\mathrm{c}};\, \boldsymbol{f}^{\mathrm{l}_1})}{\mathrm{d}\boldsymbol{p}}\boldsymbol{p}' = \mathbf{0} \Leftrightarrow \frac{\mathrm{d}(\boldsymbol{f}^{\mathrm{c}};\, \boldsymbol{f}^{\mathrm{l}_2})}{\mathrm{d}\boldsymbol{p}}\boldsymbol{p}' = \mathbf{0}.$$

Proof. As mentioned in Remark 3.2, as long as the realization is panel-wise generic, any first-order flex restricting the motion of each panel has only a rigid-body motion. Therefore, additional constraints and different choices of coplanar and length constraints do not change the space of first-order flex relating to a single panel. Since the space of first-order flex for the entire rigid origami is the intersection of the spaces of first-order flex restricting each panel, it is preserved under all different choices of coplanar constraints and length constraints. □

For the rigid origami shown in Fig 2, the size of $\mathrm{d}\boldsymbol{f}/\,\mathrm{d}\boldsymbol{p}$ is 39×36. At a panel-wise planar realization in Fig. 2(b), $\operatorname{rank}(\mathrm{d}\boldsymbol{f}/\,\mathrm{d}\boldsymbol{p}) = 27$, hence the dimension of the space of non-trivial first-order flex is 3. At 'most' non-planar panel-wise generic realizations, $\operatorname{rank}(\mathrm{d}\boldsymbol{f}/\,\mathrm{d}\boldsymbol{p}) = 30$, and the rigid origami is first-order rigid.

4. Static Rigidity

This section considers the behavior of a rigid origami from the viewpoint of static rigidity. We introduce a restricted set of external loads and internal forces that are work-conjugate to a first-order flex and an internal deformation, respectively. The idea of 'internal force' and 'internal deformation' are similar to the stress and strain in elasticity. The difference and connection are shown later in this section.

In the point-panel model, the *internal deformation* $\boldsymbol{e} \in \mathbb{R}^{n^{\mathrm{c}}+n^{\mathrm{l}}+n^{\mathrm{ca}}+n^{\mathrm{la}}}$ of a rigid origami is defined after Definition 2.2 as:

$$\boldsymbol{e} = \boldsymbol{f}(\boldsymbol{p}),\ \boldsymbol{p} \in \mathbb{R}^{3n^{\mathrm{v}}}. \tag{7}$$

That is to say:

$$\boldsymbol{e}(\boldsymbol{p}) = \boldsymbol{0} \text{ only if } \boldsymbol{p} \in \mathcal{P}. \tag{8}$$

Suppose that the rigid origami is associated with a second or higher-order differentiable strain energy $U(\boldsymbol{e}) \in \mathbb{R}$ which is only dependent on the internal deformation $\boldsymbol{e}$ and satisfies:

$$U(\boldsymbol{0}) = 0,\ U(\boldsymbol{e}) > 0 \text{ if } \boldsymbol{e} \neq \boldsymbol{0}. \tag{9}$$

In addition, suppose the rigid origami is subject to a second or higher-order differentiable scalar potential $V(\boldsymbol{p})$ which is only dependent on the position of vertices $\boldsymbol{p}$.

From the perspective of analytical mechanics, the total potential energy of the rigid origami is $U+V$. At the equilibrium state, the following equation holds:

$$\frac{\mathrm{d}(U+V)}{\mathrm{d}\boldsymbol{p}} = \frac{\mathrm{d}U}{\mathrm{d}\boldsymbol{e}}\frac{\mathrm{d}\boldsymbol{f}}{\mathrm{d}\boldsymbol{p}} + \frac{\mathrm{d}V}{\mathrm{d}\boldsymbol{p}} = \boldsymbol{0}. \tag{10}$$

Then, the internal force and load are denoted by the column vectors $\boldsymbol{\omega} \in$

$\mathbb{R}^{n^{\mathrm{c}}+n^{\mathrm{l}}+n^{\mathrm{ca}}+n^{\mathrm{la}}}$ and $\boldsymbol{l} \in \mathbb{R}^{3n^{\mathrm{v}}}$, respectively, which are defined as:

$$\boldsymbol{\omega} = \frac{\mathrm{d}U}{\mathrm{d}\boldsymbol{e}}, \ \boldsymbol{l} = -\frac{\mathrm{d}V}{\mathrm{d}\boldsymbol{p}}. \tag{11}$$

Hence, the equilibrium equation is:

$$\frac{\mathrm{d}\boldsymbol{f}}{\mathrm{d}\boldsymbol{p}}^{\mathsf{T}} \boldsymbol{\omega} = \boldsymbol{l}. \tag{12}$$

For a rigid origami $G(\boldsymbol{p})$, if there is an internal force $\boldsymbol{\omega}$ satisfying Eq. (12) for a given load $\boldsymbol{l}$, we say $G(\boldsymbol{p})$ can *resolve* load $\boldsymbol{l}$. In correspondence with the types of the constraints, $\boldsymbol{\omega}$ is decomposed as $\boldsymbol{\omega} = (\boldsymbol{\omega}^{\mathrm{c}}; \boldsymbol{\omega}^{\mathrm{l}}; \boldsymbol{\omega}^{\mathrm{ca}}; \boldsymbol{\omega}^{\mathrm{la}})$ where $\boldsymbol{\omega}^{\mathrm{c}} \in \mathbb{R}^{n^{\mathrm{c}}}$, $\boldsymbol{\omega}^{\mathrm{l}} \in \mathbb{R}^{n^{\mathrm{l}}}$, $\boldsymbol{\omega}^{\mathrm{ca}} \in \mathbb{R}^{n^{\mathrm{ca}}}$, and $\boldsymbol{\omega}^{\mathrm{la}} \in \mathbb{R}^{n^{\mathrm{la}}}$ are associated with $\boldsymbol{f}^{\mathrm{c}}$, $\boldsymbol{f}^{\mathrm{l}}$, $\boldsymbol{f}^{\mathrm{ca}}$, and $\boldsymbol{f}^{\mathrm{la}}$, respectively.

If the load $\boldsymbol{l} = \boldsymbol{0}$, the internal force is referred to as a *self-stress* $\boldsymbol{\omega}^{\mathrm{s}}$:

$$\frac{\mathrm{d}\boldsymbol{f}}{\mathrm{d}\boldsymbol{p}}^{\mathsf{T}} \boldsymbol{\omega}^{\mathrm{s}} = \boldsymbol{0}. \tag{13}$$

The internal work done by the internal force $\boldsymbol{\omega}$ with the *first-order internal deformation* $\mathrm{d}\boldsymbol{f} / \mathrm{d}\boldsymbol{p} \cdot \boldsymbol{p}'$ is zero:

$$\delta W_{\mathrm{in}} = \left\langle \boldsymbol{\omega}, \ \frac{\mathrm{d}\boldsymbol{f}}{\mathrm{d}\boldsymbol{p}} \boldsymbol{p}' \right\rangle = 0. \tag{14}$$

According to the principle of virtual work, the external work done by the load $\boldsymbol{l}$ with the first-order flex $\boldsymbol{p}'$ is also zero:

$$\delta W_{\mathrm{ex}} = \langle \boldsymbol{l},\ \boldsymbol{p}' \rangle = 0. \tag{15}$$

Proposition 4.1. (Invariance of the load that can be resolved) At a panel-wise generic realization, different choices of coplanar or length constraints have no effect on the space of load that can be resolved, while can only change the internal force distribution. Note that additional coplanar and length constraints increase the dimension of internal force:

(1) Additional coplanar and length constraints do not change the load that can be resolved. In other words, there is an internal force $\boldsymbol{\omega} \in \mathbb{R}^{n^{\mathrm{c}}+n^{\mathrm{l}}+n^{\mathrm{ca}}+n^{\mathrm{la}}}$ that can resolve a load $\boldsymbol{l} \in \mathbb{R}^{3n^{\mathrm{v}}}$ if and only if there is a pair of internal forces $\boldsymbol{\omega}^{\mathrm{c}} \in \mathbb{R}^{n^{\mathrm{c}}}$ and $\boldsymbol{\omega}^{\mathrm{l}} \in \mathbb{R}^{n^{\mathrm{l}}}$ that can resolve $\boldsymbol{l}$:

$$\frac{\mathrm{d}\boldsymbol{f}}{\mathrm{d}\boldsymbol{p}}^{\mathsf{T}} \boldsymbol{\omega} = \boldsymbol{l} \Leftrightarrow \frac{\mathrm{d}(\boldsymbol{f}^{\mathrm{c}};\ \boldsymbol{f}^{\mathrm{l}})}{\mathrm{d}\boldsymbol{p}}^{\mathsf{T}} (\boldsymbol{\omega}^{\mathrm{c}};\ \boldsymbol{\omega}^{\mathrm{l}}) = \boldsymbol{l}.$$

(2) Different choices of vertices for elementary coplanar constraints do not change the load that can be resolved. In other words, suppose there are two choices of coplanar constraints $\boldsymbol{f}^{\mathrm{c}_1}$ and $\boldsymbol{f}^{\mathrm{c}_2}$, there is an internal force $\boldsymbol{\omega}^{\mathrm{c}_1} \in \mathbb{R}^{n^{\mathrm{c}}}$ that can resolve a load $\boldsymbol{l} \in \mathbb{R}^{3n^{\mathrm{v}}}$ with $\boldsymbol{\omega}^{\mathrm{l}} \in \mathbb{R}^{n^{\mathrm{l}}}$ if and only if there is an internal force $\boldsymbol{\omega}^{\mathrm{c}_2} \in \mathbb{R}^{n^{\mathrm{c}}}$ that can resolve $\boldsymbol{l}$ with $\boldsymbol{\omega}^{\mathrm{l}}$:

$$\frac{\mathrm{d}(\boldsymbol{f}^{\mathrm{c}_1};\ \boldsymbol{f}^{\mathrm{l}})}{\mathrm{d}\boldsymbol{p}}^{\mathsf{T}} (\boldsymbol{\omega}^{\mathrm{c}_1};\ \boldsymbol{\omega}^{\mathrm{l}}) = \boldsymbol{l} \Leftrightarrow \frac{\mathrm{d}(\boldsymbol{f}^{\mathrm{c}_2};\ \boldsymbol{f}^{\mathrm{l}})}{\mathrm{d}\boldsymbol{p}}^{\mathsf{T}} (\boldsymbol{\omega}^{\mathrm{c}_2};\ \boldsymbol{\omega}^{\mathrm{l}}) = \boldsymbol{l}.$$

(3) Different choices of diagonals for elementary length constraints do not change the load that can be resolved. In other words, suppose there are two choices of diagonals to form the elementary length constraints $\boldsymbol{f}^{\mathrm{l}_1}$ and $\boldsymbol{f}^{\mathrm{l}_2}$, there is an internal force $\boldsymbol{\omega}^{\mathrm{l}_1} \in \mathbb{R}^{n^{\mathrm{l}}}$ that can resolve a load $\boldsymbol{l} \in \mathbb{R}^{3n^{\mathrm{v}}}$ with $\boldsymbol{\omega}^{\mathrm{c}} \in \mathbb{R}^{n^{\mathrm{c}}}$ if and only if there is an internal force $\boldsymbol{\omega}^{\mathrm{l}_2} \in \mathbb{R}^{n^{\mathrm{l}}}$ that can resolve $\boldsymbol{l}$ with $\boldsymbol{\omega}^{\mathrm{c}}$:

$$\frac{\mathrm{d}(\boldsymbol{f}^{\mathrm{c}};\, \boldsymbol{f}^{\mathrm{l}_1})}{\mathrm{d}\boldsymbol{p}}^{\mathsf{T}}(\boldsymbol{\omega}^{\mathrm{c}};\, \boldsymbol{\omega}^{\mathrm{l}_1}) = \boldsymbol{l} \Leftrightarrow \frac{\mathrm{d}(\boldsymbol{f}^{\mathrm{c}};\, \boldsymbol{f}^{\mathrm{l}_2})}{\mathrm{d}\boldsymbol{p}}^{\mathsf{T}}(\boldsymbol{\omega}^{\mathrm{c}};\, \boldsymbol{\omega}^{\mathrm{l}_2}) = \boldsymbol{l}.$$

Proof. From Eq. (15), the space of load that can be resolved is the orthogonal complement of the space of first-order flex, which is invariant to different choices of coplanar or length constraints as shown in Proposition 3.3. Therefore, the space of load that can be resolved is also invariant to different choices of coplanar or length constraints. In other words, the load can be resolved only by the components of $\boldsymbol{\omega}$ corresponding to the predefined elementary coplanar and length constraints, and the remaining components of $\boldsymbol{\omega}$ form the self-stress.

Next, we explain how the distribution of internal forces changes with the additional coplanar and length constraints or the different choices of vertices of elementary coplanar constraints or diagonals of elementary length constraints. First, the change of the internal force distribution for the additional coplanar and length constraints is shown. Suppose there is an $\boldsymbol{\omega}_1$ in the elementary and additional constraints that can resolve $\boldsymbol{l}$, then $\boldsymbol{\omega}_1$ could be decomposed as described in the following equation:

$$\begin{aligned}\boldsymbol{\omega}_1 &= (\boldsymbol{\omega}_1^{\mathrm{c}};\, \boldsymbol{\omega}_1^{\mathrm{l}};\, \boldsymbol{\omega}_1^{\mathrm{ca}};\, \boldsymbol{\omega}_1^{\mathrm{la}}) \\ &= (\boldsymbol{\omega}_1^{\mathrm{c}} - \boldsymbol{\omega}_2^{\mathrm{c}};\, \boldsymbol{\omega}_1^{\mathrm{l}} - \boldsymbol{\omega}_2^{\mathrm{l}};\, \mathbf{0}^{\mathrm{ca}};\, \mathbf{0}^{\mathrm{la}}) + (\boldsymbol{\omega}_2^{\mathrm{c}};\, \boldsymbol{\omega}_2^{\mathrm{l}};\, \boldsymbol{\omega}_1^{\mathrm{ca}};\, \boldsymbol{\omega}_1^{\mathrm{la}}),\end{aligned} \tag{16}$$

where $\boldsymbol{\omega}_2^{\mathrm{c}}$ and $\boldsymbol{\omega}_2^{\mathrm{l}}$ make the second term in the right-hand side of Eq. (16) a self-stress. In the following, such decomposition is referred to as a *transition* between internal forces in different choice of diagonals. Similarly, suppose $(\boldsymbol{\omega}_1^{\mathrm{c}};\, \boldsymbol{\omega}_1^{\mathrm{l}};\, \mathbf{0}^{\mathrm{ca}};\, \mathbf{0}^{\mathrm{la}})$ can resolve $\boldsymbol{l}$ in a set of elementary coplanar constraints, we have the transition between different choices of elementary coplanar constraints described as:

$$\begin{aligned}(\boldsymbol{\omega}_1^{\mathrm{c}_1};\, \boldsymbol{\omega}_1^{\mathrm{l}};\, \mathbf{0}^{\mathrm{ca}_1}) &= (\boldsymbol{\omega}_1^{\mathrm{c}_1} + \boldsymbol{\omega}_2^{\mathrm{c}_1};\, \boldsymbol{\omega}_1^{\mathrm{l}};\, \boldsymbol{\omega}_1^{\mathrm{ca}_1}) - (\boldsymbol{\omega}_2^{\mathrm{c}_1};\, \mathbf{0}^{\mathrm{l}};\, \boldsymbol{\omega}_1^{\mathrm{ca}_1}) \\ &= (\boldsymbol{\omega}_1^{\mathrm{c}_2};\, \boldsymbol{\omega}_1^{\mathrm{l}};\, \boldsymbol{\omega}_1^{\mathrm{ca}_2}) - (\boldsymbol{\omega}_2^{\mathrm{c}_1};\, \mathbf{0}^{\mathrm{l}};\, \boldsymbol{\omega}_1^{\mathrm{ca}_1}) \\ &= (\boldsymbol{\omega}_1^{\mathrm{c}_2} - \boldsymbol{\omega}_2^{\mathrm{c}_2};\, \boldsymbol{\omega}_1^{\mathrm{l}};\, \mathbf{0}^{\mathrm{ca}_2}) + (\boldsymbol{\omega}_2^{\mathrm{c}_2};\, \mathbf{0}^{\mathrm{l}};\, \boldsymbol{\omega}_1^{\mathrm{ca}_2}) - (\boldsymbol{\omega}_2^{\mathrm{c}_1};\, \mathbf{0}^{\mathrm{l}};\, \boldsymbol{\omega}_1^{\mathrm{ca}_1}),\end{aligned} \tag{17}$$

where $\boldsymbol{\omega}_1^{\mathrm{c}_2}$ and $\boldsymbol{\omega}_1^{\mathrm{ca}_2}$ satisfy:

$$\frac{\mathrm{d}(\boldsymbol{f}^{\mathrm{c}_2};\, \boldsymbol{f}^{\mathrm{ca}_2})}{\mathrm{d}\boldsymbol{p}}^{\mathsf{T}}(\boldsymbol{\omega}_1^{\mathrm{c}_2};\, \boldsymbol{\omega}_1^{\mathrm{ca}_2}) = \frac{\mathrm{d}(\boldsymbol{f}^{\mathrm{c}_1};\, \boldsymbol{f}^{\mathrm{ca}_1})}{\mathrm{d}\boldsymbol{p}}^{\mathsf{T}}(\boldsymbol{\omega}_1^{\mathrm{c}_1} + \boldsymbol{\omega}_2^{\mathrm{c}_1};\, \boldsymbol{\omega}_1^{\mathrm{ca}_1}) \tag{18}$$

for the additional coplanar constraints $\boldsymbol{f}^{\mathrm{ca}}$. $\boldsymbol{\omega}_2^{\mathrm{c}_1}$ and $\boldsymbol{\omega}_2^{\mathrm{c}_2}$ makes the second and third terms in the right-hand side of Eq. (17) self-stresses. There is also a similar transition between internal forces in different choices of elementary length constraints described as follows:

$$
\begin{aligned}
(\boldsymbol{\omega}_1^{\mathrm{c}};\, \boldsymbol{\omega}_1^{\mathrm{l}_1};\, \mathbf{0}^{\mathrm{la}_1}) &= (\boldsymbol{\omega}_1^{\mathrm{c}};\, \boldsymbol{\omega}_1^{\mathrm{l}_1} + \boldsymbol{\omega}_2^{\mathrm{l}_1};\, \boldsymbol{\omega}_1^{\mathrm{la}_1}) - (\mathbf{0}^{\mathrm{c}};\, \boldsymbol{\omega}_2^{\mathrm{l}_1};\, \boldsymbol{\omega}_1^{\mathrm{la}_1}) \\
&= (\boldsymbol{\omega}_1^{\mathrm{c}};\, \boldsymbol{\omega}_1^{\mathrm{l}_2};\, \boldsymbol{\omega}_1^{\mathrm{la}_2}) - (\mathbf{0}^{\mathrm{c}};\, \boldsymbol{\omega}_2^{\mathrm{l}_1};\, \boldsymbol{\omega}_1^{\mathrm{la}_1}) \\
&= (\boldsymbol{\omega}_1^{\mathrm{c}};\, \boldsymbol{\omega}_1^{\mathrm{c}_2} - \boldsymbol{\omega}_2^{\mathrm{l}_2};\, \mathbf{0}^{\mathrm{la}_2}) + (\mathbf{0}^{\mathrm{c}};\, \boldsymbol{\omega}_2^{\mathrm{l}_2};\, \boldsymbol{\omega}_1^{\mathrm{la}_2}) - (\mathbf{0}^{\mathrm{c}};\, \boldsymbol{\omega}_2^{\mathrm{l}_1};\, \boldsymbol{\omega}_1^{\mathrm{la}_1}),
\end{aligned} \tag{19}
$$

where $\boldsymbol{\omega}_1^{\mathrm{l}_2}$ and $\boldsymbol{\omega}_1^{\mathrm{la}_2}$ satisfy:

$$
\frac{\mathrm{d}(\boldsymbol{f}^{\mathrm{l}_2};\, \boldsymbol{f}^{\mathrm{la}_2})}{\mathrm{d}\boldsymbol{p}}^{\mathsf{T}} (\boldsymbol{\omega}_1^{\mathrm{l}_2};\, \boldsymbol{\omega}_1^{\mathrm{la}_2}) = \frac{\mathrm{d}(\boldsymbol{f}^{\mathrm{l}_1};\, \boldsymbol{f}^{\mathrm{la}_1})}{\mathrm{d}\boldsymbol{p}}^{\mathsf{T}} (\boldsymbol{\omega}_1^{\mathrm{l}_1} + \boldsymbol{\omega}_2^{\mathrm{l}_1};\, \boldsymbol{\omega}_1^{\mathrm{la}_1}). \tag{20}
$$

$\boldsymbol{\omega}_2^{\mathrm{l}_1}$ and $\boldsymbol{\omega}_2^{\mathrm{l}_2}$ makes the second and third terms in the right-hand side of Eq. (19) self-stresses. □

Definition 4.2. A rigid origami is *statically rigid* if it can resolve every load. A rigid origami is *independent* if there is only zero self-stress. A rigid origami is *isostatic* if it is first-order rigid and independent.

Theorem 4.3. (1) A rigid origami is statically rigid if and only if it is first-order rigid.

(2) (Maxwell count) If the dimension of the space of first-order flex and self-stress are denoted by n^{f} and n^{s}, respectively, then:

$$
n^{\mathrm{f}} - n^{\mathrm{s}} = 3n^{\mathrm{v}} - (n^{\mathrm{c}} + n^{\mathrm{l}} + n^{\mathrm{ca}} + n^{\mathrm{la}}). \tag{21}
$$

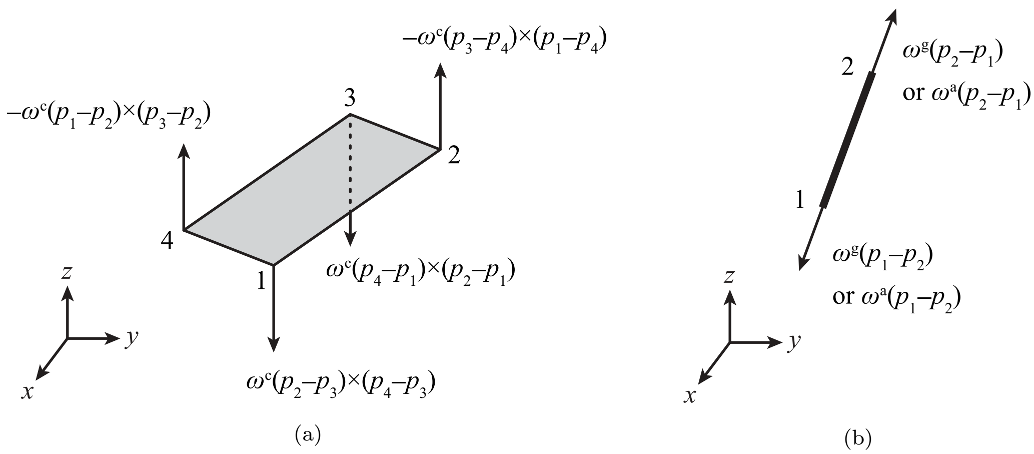

Figure 4: (a) Forces at vertices obtained from the internal force corresponding to the coplanar constraint for a panel. (b) Forces at vertices obtained from the internal force corresponding to the length constraint for a boundary line or a diagonal.

In the rest of this section, the physical meanings of load $\boldsymbol{l}$, first-order internal deformation $\mathrm{d}\boldsymbol{e} = \mathrm{d}\boldsymbol{f} \,/\, \mathrm{d}\boldsymbol{p} \cdot \boldsymbol{p}'$, and internal force $\boldsymbol{\omega}$ are clarified. A load $\boldsymbol{l}$ is the work conjugate of a first-order flex $\boldsymbol{p}'$, hence is in the form of concentrated force on each vertex.

Here, the physical meanings of first-order internal deformation and internal force are explained in simplified forms. Suppose vertices 1, 2, 3, 4 are coplanar, the first-order internal deformation $\mathrm{d}e^{\mathrm{c}} \in \mathbb{R}$ for the coplanar constraint over $p_1,\ p_2,\ p_3,\ p_4$ is:

$$
\begin{aligned}
\mathrm{d}e^{\mathrm{c}} =& \frac{\mathrm{d}f^{\mathrm{c}}(1,\,2,\,3,\,4)}{\mathrm{d}(p_1;\,p_2;\,p_3;\,p_4)}(p_1';\,p_2';\,p_3';\,p_4') \\
=& \langle (p_2-p_3)\times(p_4-p_3),\ p_1'\rangle - \langle (p_3-p_4)\times(p_1-p_4),\ p_2'\rangle \\
&+ \langle (p_4-p_1)\times(p_2-p_1),\ p_3'\rangle - \langle (p_1-p_2)\times(p_3-p_2),\ p_4'\rangle\,.
\end{aligned} \tag{22}
$$

It means that the internal force $\omega^{\mathrm{c}} \in \mathbb{R}$ for each coplanar constraint, which is defined as the work-conjugate of a first-order internal deformation, is a uniform pressure. $\mathrm{d}f^{\mathrm{c}}(1,\, \ldots,\, 4) \,/\, \mathrm{d}(p_1;\, \ldots;\, p_4)^{\mathsf{T}}\omega^{\mathrm{c}}$ is hence in the form of concentrated force on corresponding vertices perpendicular to the panel (Fig. 4(a)):

$$\frac{\mathrm{d}f^{\mathrm{c}}(1,\, 2,\, 3,\, 4)}{\mathrm{d}(p_1;\, p_2;\, p_3;\, p_4)}^{\mathsf{T}} \omega^{\mathrm{c}} = \begin{bmatrix} (p_2 - p_3) \times (p_4 - p_3) \\ (p_3 - p_4) \times (p_1 - p_4) \\ (p_4 - p_1) \times (p_2 - p_1) \\ (p_1 - p_2) \times (p_3 - p_2) \end{bmatrix} \omega^{\mathrm{c}}. \tag{23}$$

Suppose there is a length constraint between vertices $1,\ 2$, the first-order internal deformation $\mathrm{d}e^{\mathrm{l}} \in \mathbb{R}$ for the length constraint over p_1 and p_2 is:

$$\mathrm{d}e^{\mathrm{l}} = \frac{\mathrm{d}f^{\mathrm{l}}(1,\, 2)}{\mathrm{d}(p_1;\, p_2)}(p_1';\, p_2') = \left\langle p_1 - p_2,\ p_1' - p_2' \right\rangle . \tag{24}$$

It means that the internal force $\omega^{\mathrm{l}} \in \mathbb{R}$ for each length constraint is an axial force per unit length which is often referred to as a 'force density' [24]. $\mathrm{d}f^{\mathrm{l}}(1,\, 2) \,/\, \mathrm{d}(p_1;\, p_2)^{\mathsf{T}}\omega^{\mathrm{l}}$ is hence in the form of concentrated force on corresponding vertices parallel to the boundary line or diagonal (Fig. 4(b)):

$$\frac{\mathrm{d}f^{\mathrm{l}}(1,\, 2)}{\mathrm{d}(p_1;\, p_2)}^{\mathsf{T}} \omega^{\mathrm{l}} = \begin{bmatrix} p_1 - p_2 \\ p_2 - p_1 \end{bmatrix} \omega^{\mathrm{l}} \quad \text{or} \quad \frac{\mathrm{d}f^{\mathrm{a}}(1,\, 2)}{\mathrm{d}(p_1;\, p_2)}^{\mathsf{T}} \omega^{\mathrm{a}} = \begin{bmatrix} p_1 - p_2 \\ p_2 - p_1 \end{bmatrix} \omega^{\mathrm{a}}. \tag{25}$$

5. Prestress stability

This section considers a rigid origami that is not first-order rigid, but is rigid, and elucidates how the stability of these structures is changed when prestress or load is added. For these purposes, we carry out the second-order analysis of the total potential energy $U+V$ introduced at the beginning of Section 4.

5.1. Unloaded case

Assume U and V have continuous second-order partial derivatives, the second-order differential (or the Hessian matrix) of $U+V$ with respect to the coordinates of vertices is written as follows with a slight abuse of notation for a product of a tensor and a vector:

$$\frac{\mathrm{d}^2(U+V)}{\mathrm{d}\boldsymbol{p}^2} = \frac{\mathrm{d}\boldsymbol{f}}{\mathrm{d}\boldsymbol{p}}^{\top} \frac{\mathrm{d}^2 U}{\mathrm{d}\boldsymbol{e}^2} \frac{\mathrm{d}\boldsymbol{f}}{\mathrm{d}\boldsymbol{p}} + \frac{\mathrm{d}U}{\mathrm{d}\boldsymbol{e}} \frac{\mathrm{d}^2\boldsymbol{f}}{\mathrm{d}\boldsymbol{p}^2} + \frac{\mathrm{d}^2 V}{\mathrm{d}\boldsymbol{p}^2}, \tag{26}$$

where $d^2U \,/\, d\boldsymbol{e}^2$ and $d^2V \,/\, d\boldsymbol{p}^2$ are the Hessian matrix of U and V with respect to $\boldsymbol{e}$ and $\boldsymbol{p}$, respectively. The Hessian of constraints $\mathrm{d}^2\boldsymbol{f} \,/\, \mathrm{d}\boldsymbol{p}^2$ is an order 3 tensor with dimension $(n^{\mathrm{c}}+n^{\mathrm{l}}+n^{\mathrm{ca}}+n^{\mathrm{la}}) \times 3n^{\mathrm{v}} \times 3n^{\mathrm{v}}$. Each component of this Hessian $\mathrm{d}^2 f_k \,/\, \mathrm{d}\boldsymbol{p}^2 \in \mathbb{R}^{3n^{\mathrm{v}} \times 3n^{\mathrm{v}}}$ $(k \in \mathbb{Z}^+,\ k \leq n^{\mathrm{c}} + n^{\mathrm{l}} + n^{\mathrm{ca}} + n^{\mathrm{la}})$ is the Hessian matrix for a single coplanar or length constraint denoted by f_k. Since $\boldsymbol{l} = -\mathrm{d}V \,/\, \mathrm{d}\boldsymbol{p}$, Eq. (26) can be rewritten as follows:

$$\frac{\mathrm{d}^2(U+V)}{\mathrm{d}\boldsymbol{p}^2} = \frac{\mathrm{d}\boldsymbol{f}}{\mathrm{d}\boldsymbol{p}}^{\top} \frac{\mathrm{d}^2 U}{\mathrm{d}\boldsymbol{e}^2} \frac{\mathrm{d}\boldsymbol{f}}{\mathrm{d}\boldsymbol{p}} + \frac{\mathrm{d}U}{\mathrm{d}\boldsymbol{e}} \frac{\mathrm{d}^2\boldsymbol{f}}{\mathrm{d}\boldsymbol{p}^2} - \frac{\mathrm{d}\boldsymbol{l}}{\mathrm{d}\boldsymbol{p}}. \tag{27}$$

A sufficient condition for $U+V$ to be strictly local minimum at an equilibrium state, which implies that the equilibrium state is stable, is that $\mathrm{d}^2(U+V)\,/\,\mathrm{d}\boldsymbol{p}^2$ is positive definite for any nonzero perturbation $\delta\boldsymbol{p}$:

$$\delta\boldsymbol{p}^{\mathsf{T}}\frac{\mathrm{d}^2(U+V)}{\mathrm{d}\boldsymbol{p}^2}\delta\boldsymbol{p} > 0 \quad \text{for any nonzero } \delta\boldsymbol{p} \in \mathbb{R}^{3n^{\mathrm{v}}}. \tag{28}$$

The above derivation shows how $\mathrm{d}^2(U+V)\,/\,\mathrm{d}\boldsymbol{p}^2$ works as the 'stiffness' of a rigid origami. However, if the variation $\delta(U+V)=0$ for a perturbation $\delta\boldsymbol{p}$, higher order information of energy might be necessary to determine the stability along this perturbation.

Furthermore, $\mathrm{d}^2U\,/\,\mathrm{d}\boldsymbol{e}^2$ is positive definite in Eq. (26) from the requirement in Eq. (9):

$$\delta\boldsymbol{e}^{\mathsf{T}}\frac{\mathrm{d}^2U}{\mathrm{d}\boldsymbol{e}^2}\delta\boldsymbol{e} > 0 \quad \text{for any nonzero } \delta\boldsymbol{e} \in \mathbb{R}^{n^{\mathrm{c}}+n^{\mathrm{l}}+n^{\mathrm{ca}}+n^{\mathrm{la}}}, \tag{29}$$

where $\delta\boldsymbol{e}$ is the variation of $\boldsymbol{e}$ due to the perturbation $\delta\boldsymbol{p}$. For an infinitesimal $\delta\boldsymbol{p}$, $\delta\boldsymbol{e} = \mathrm{d}\boldsymbol{f}\,/\,\mathrm{d}\boldsymbol{p}\cdot\delta\boldsymbol{p}$ at a realization $\boldsymbol{p}$, and the first term in the right-hand side of Eq. (26) is positive semidefinite:

$$\begin{aligned}
&\delta\boldsymbol{p}^{\mathsf{T}}\frac{\mathrm{d}\boldsymbol{f}}{\mathrm{d}\boldsymbol{p}}^{\mathsf{T}}\frac{\mathrm{d}^2U}{\mathrm{d}\boldsymbol{e}^2}\frac{\mathrm{d}\boldsymbol{f}}{\mathrm{d}\boldsymbol{p}}\delta\boldsymbol{p} \geq 0 \quad \text{for any nonzero } \delta\boldsymbol{p} \in \mathbb{R}^{3n^{\mathrm{v}}},\\
&\delta\boldsymbol{p}^{\mathsf{T}}\frac{\mathrm{d}\boldsymbol{f}}{\mathrm{d}\boldsymbol{p}}^{\mathsf{T}}\frac{\mathrm{d}^2U}{\mathrm{d}\boldsymbol{e}^2}\frac{\mathrm{d}\boldsymbol{f}}{\mathrm{d}\boldsymbol{p}}\delta\boldsymbol{p} = 0 \quad \text{only if } \delta\boldsymbol{p} \text{ is a nonzero first-order flex.}
\end{aligned} \tag{30}$$

In this subsection, the prestress stability is discussed assuming there is no load ($\mathrm{d}V\,/\,\mathrm{d}\boldsymbol{p}=\boldsymbol{0}$).

Definition 5.1. At a realization $\boldsymbol{p}$, a rigid origami $G(\boldsymbol{p})$ is *prestress stable* if there is a positive definite matrix $\boldsymbol{E} \in \mathbb{R}^{(n^{\mathrm{c}}+n^{\mathrm{l}}+n^{\mathrm{ca}}+n^{\mathrm{la}})\times(n^{\mathrm{c}}+n^{\mathrm{l}}+n^{\mathrm{ca}}+n^{\mathrm{la}})}$ and a vector $\boldsymbol{\omega}^{\mathrm{s}} \in \mathbb{R}^{n^{\mathrm{c}}+n^{\mathrm{l}}+n^{\mathrm{ca}}+n^{\mathrm{la}}}$ such that:

$$\frac{\mathrm{d}\boldsymbol{f}}{\mathrm{d}\boldsymbol{p}}^{\top}\boldsymbol{\omega}^{\mathrm{s}} = \boldsymbol{0} \tag{31}$$

and

$$\boldsymbol{K} = \frac{\mathrm{d}\boldsymbol{f}}{\mathrm{d}\boldsymbol{p}}^{\top}\boldsymbol{E}\frac{\mathrm{d}\boldsymbol{f}}{\mathrm{d}\boldsymbol{p}} + \boldsymbol{\omega}^{\mathrm{s}}\cdot\frac{\mathrm{d}^2\boldsymbol{f}}{\mathrm{d}\boldsymbol{p}^2} \tag{32}$$

is positive-definite where $\boldsymbol{\omega}^{\mathrm{s}}\cdot\mathrm{d}^2\boldsymbol{f}\,/\,\mathrm{d}\boldsymbol{p}^2 \in \mathbb{R}^{3n^{\mathrm{v}}\times 3n^{\mathrm{v}}}$ is the sum of $\omega^{\mathrm{s}}_k[\mathrm{d}^2 f_k\,/\,\mathrm{d}\boldsymbol{p}^2] \in \mathbb{R}^{3n^{\mathrm{v}}\times 3n^{\mathrm{v}}}$ for all $k \in \mathbb{Z}^+,\ k \le n^{\mathrm{c}}+n^{\mathrm{l}}+n^{\mathrm{ca}}+n^{\mathrm{la}}$.

Physically, $\boldsymbol{E}$ is the *local elasticity matrix*, which is the Hessian of the predefined energy function. $\boldsymbol{K}$ is the *tangent stiffness matrix* or *total stiffness matrix*. $\boldsymbol{\omega}^{\mathrm{s}}\cdot\mathrm{d}^2\boldsymbol{f}\,/\,\mathrm{d}\boldsymbol{p}^2$ or $\boldsymbol{\omega}\cdot\mathrm{d}^2\boldsymbol{f}\,/\,\mathrm{d}\boldsymbol{p}^2$ is called the *stress matrix*. We say a self-stress $\boldsymbol{\omega}^{\mathrm{s}}$ or an internal force $\boldsymbol{\omega}$ *stabilizes* a rigid origami if it leads to a positive definite stiffness $\boldsymbol{K}$.

Proposition 5.2. (Stress test) At a realization $\boldsymbol{p}$, a rigid origami $G(\boldsymbol{p})$ is prestress stable if and only if there is a self-stress $\boldsymbol{\omega}^{\mathrm{s}} \in \mathbb{R}^{n^{\mathrm{c}}+n^{\mathrm{l}}+n^{\mathrm{ca}}+n^{\mathrm{la}}}$ such that the stress matrix $\boldsymbol{\omega}^{\mathrm{s}}\cdot\mathrm{d}^2\boldsymbol{f}\,/\,\mathrm{d}\boldsymbol{p}^2$ is positive definite over the space of first-order flex:

$$\boldsymbol{p}'^{\top}\left(\boldsymbol{\omega}^{\mathrm{s}}\cdot\frac{\mathrm{d}^2\boldsymbol{f}}{\mathrm{d}\boldsymbol{p}^2}\right)\boldsymbol{p}' = \left\langle \boldsymbol{\omega}^{\mathrm{s}},\, \boldsymbol{p}'^{\top}\frac{\mathrm{d}^2\boldsymbol{f}}{\mathrm{d}\boldsymbol{p}^2}\boldsymbol{p}'\right\rangle > 0 \quad \text{for any first-order flex } \boldsymbol{p}', \tag{33}$$

where $\boldsymbol{p}'^{\top}[\mathrm{d}^2\boldsymbol{f}\,/\,\mathrm{d}\boldsymbol{p}^2]\boldsymbol{p}'$ is an $n^{\mathrm{c}}+n^{\mathrm{l}}+n^{\mathrm{ca}}+n^{\mathrm{la}}$ column vector whose k-th component is $\boldsymbol{p}'^{\mathsf{T}}[\mathrm{d}^2 f_k \,/\, \mathrm{d}\boldsymbol{p}^2]\boldsymbol{p}'$ $(k \in \mathbb{Z}^+,\ k \leq n^{\mathrm{c}} + n^{\mathrm{l}} + n^{\mathrm{ca}} + n^{\mathrm{la}})$.

Proof. Necessity: if $G(\boldsymbol{p})$ is prestress stable, the quadratic form of a first-order flex in the left-hand side of Eq. (33) should be greater than zero, hence the stress matrix is positive definite over the space of first-order flex.

Sufficiency: We show that if there exists a self stress $\boldsymbol{\omega}^{\mathrm{s}}$ such that $\boldsymbol{\omega}^{\mathrm{s}} \cdot \mathrm{d}^2\boldsymbol{f} \,/\, \mathrm{d}\boldsymbol{p}^2$ is positive definite over the space of first-order flex,

$$\boldsymbol{K}(\gamma) = \frac{\mathrm{d}\boldsymbol{f}}{\mathrm{d}\boldsymbol{p}}^{\mathsf{T}} \boldsymbol{E} \frac{\mathrm{d}\boldsymbol{f}}{\mathrm{d}\boldsymbol{p}} + \gamma \boldsymbol{\omega}^{\mathrm{s}} \cdot \frac{\mathrm{d}^2\boldsymbol{f}}{\mathrm{d}\boldsymbol{p}^2} \tag{34}$$

would be positive definite by choosing a sufficiently small $\gamma > 0$. First, consider the case where a perturbation $\delta\boldsymbol{p}$ is a first-order flex. In this case, clearly $\delta\boldsymbol{p}^{\mathsf{T}}\boldsymbol{K}(\gamma)\delta\boldsymbol{p} > 0$ for any $\gamma > 0$. Next, consider the case where $\delta\boldsymbol{p}$ is not a first-order flex. Here, suppose the Euclidean norm of $\delta\boldsymbol{p}$ is $\|\delta\boldsymbol{p}\| = 1$. Since the set of $\delta\boldsymbol{p}$ with $\|\delta\boldsymbol{p}\| = 1$ is compact, the expression below has a positive lower bound, i.e., there exists $\varepsilon > 0$ such that:

$$\delta\boldsymbol{p}^{\mathsf{T}} \frac{\mathrm{d}\boldsymbol{f}}{\mathrm{d}\boldsymbol{p}}^{\mathsf{T}} \boldsymbol{E} \frac{\mathrm{d}\boldsymbol{f}}{\mathrm{d}\boldsymbol{p}} \delta\boldsymbol{p} \geq \varepsilon, \tag{35}$$

and we have

$$\delta\boldsymbol{p}^{\mathsf{T}} \left[\boldsymbol{\omega}^{\mathrm{s}} \cdot \frac{\mathrm{d}^2\boldsymbol{f}}{\mathrm{d}\boldsymbol{p}^2}\right] \delta\boldsymbol{p} \geq - \left\|\boldsymbol{\omega}^{\mathrm{s}} \cdot \frac{\mathrm{d}^2\boldsymbol{f}}{\mathrm{d}\boldsymbol{p}^2}\right\|, \tag{36}$$

where $\|\boldsymbol{\omega}^{\mathrm{s}} \cdot \mathrm{d}^2\boldsymbol{f} \,/\, \mathrm{d}\boldsymbol{p}^2\|$ is the matrix norm. Then, we can choose:

$$0 < \gamma < \frac{\varepsilon}{\left\| \boldsymbol{\omega}^{\mathrm{s}} \cdot \dfrac{\mathrm{d}^2\boldsymbol{f}}{\mathrm{d}\boldsymbol{p}^2} \right\|} \tag{37}$$

so that $\delta\boldsymbol{p}^{\mathsf{T}}\boldsymbol{K}(\gamma)\delta\boldsymbol{p} > 0$ for any $\delta\boldsymbol{p}$ with $\|\delta\boldsymbol{p}\| = 1$. Furthermore, when $\|\delta\boldsymbol{p}\| \neq 1$, we could choose the same γ for $\delta\boldsymbol{p} \,/\, \|\delta\boldsymbol{p}\|$. □

Corollary 5.3. When the dimension of non-trivial first-order flex is $n^{\mathrm{f}} > 0$, the bases of the space of first-order flex are denoted by $\bar{\boldsymbol{p}}'_1, \ \bar{\boldsymbol{p}}'_2, \ \ldots, \ \bar{\boldsymbol{p}}'_{n^{\mathrm{f}}} \in \mathbb{R}^{3n^{\mathrm{v}}}$, and these bases are assembled into a $3n^{\mathrm{v}} \times n^{\mathrm{f}}$ matrix as:

$$\bar{\boldsymbol{P}}' = [\bar{\boldsymbol{p}}'_1 \ \ \bar{\boldsymbol{p}}'_2 \ \ \cdots \ \ \bar{\boldsymbol{p}}'_{n^{\mathrm{f}}}]\,. \tag{38}$$

From Proposition 5.2, a rigid origami $G(\boldsymbol{p})$ is prestress stable if and only if:

$$\bar{\boldsymbol{P}}'^{\mathsf{T}} \left[\boldsymbol{\omega}^{\mathrm{s}} \cdot \frac{\mathrm{d}^2\boldsymbol{f}}{\mathrm{d}\boldsymbol{p}^2}\right] \bar{\boldsymbol{P}}' \in \mathbb{R}^{n^{\mathrm{f}} \times n^{\mathrm{f}}} \quad \text{is positive definite.} \tag{39}$$

Proposition 5.4. (Invariance of prestress stability) At a panel-wise generic realization, different choices of coplanar or length constraints have no effect on the prestress stability:

(1) Additional constraints do not change the prestress stability. In other words, there is a self-stress $\boldsymbol{\omega}^{\mathrm{s}} \in \mathbb{R}^{n^{\mathrm{c}}+n^{\mathrm{l}}+n^{\mathrm{ca}}+n^{\mathrm{la}}}$ that can stabilize the rigid origami $G(\boldsymbol{p})$ if and only if there is a pair of self-stresses $\boldsymbol{\omega}^{\mathrm{sc}} \in \mathbb{R}^{n^{\mathrm{c}}}$

and $\boldsymbol{\omega}^{\mathrm{sl}} \in \mathbb{R}^{n^{\mathrm{l}}}$ that can stabilize $G(\boldsymbol{p})$:

$$\boldsymbol{p}'^{\mathsf{T}} \left[\boldsymbol{\omega}^{\mathrm{s}} \cdot \frac{\mathrm{d}^2 \boldsymbol{f}}{\mathrm{d}\boldsymbol{p}^2}\right] \boldsymbol{p}' > 0 \Leftrightarrow \boldsymbol{p}'^{\mathsf{T}} \left[(\boldsymbol{\omega}^{\mathrm{sc}};\, \boldsymbol{\omega}^{\mathrm{sl}}) \cdot \frac{\mathrm{d}^2(\boldsymbol{f}^{\mathrm{c}};\, \boldsymbol{f}^{\mathrm{l}})}{\mathrm{d}\boldsymbol{p}^2}\right] \boldsymbol{p}' > 0$$
$$\text{for any first-order flex } \boldsymbol{p}'.$$

(2) Different choices of vertices for elementary coplanar constraints do not change the prestress stability. In other words, suppose there are two choices of coplanar constraints $\boldsymbol{f}^{\mathrm{c}_1}$ and $\boldsymbol{f}^{\mathrm{c}_2}$, there is a self-stress $\boldsymbol{\omega}^{\mathrm{sc}_1} \in \mathbb{R}^{n^{\mathrm{c}}}$ that can stabilize the rigid origami $G(\boldsymbol{p})$ with $\boldsymbol{\omega}^{\mathrm{sl}} \in \mathbb{R}^{n^{\mathrm{l}}}$ if and only if there is a self-stress $\boldsymbol{\omega}^{\mathrm{sc}_2} \in \mathbb{R}^{n^{\mathrm{c}}}$ that can stabilize the rigid origami $G(\boldsymbol{p})$ with $\boldsymbol{\omega}^{\mathrm{sl}}$:

$$\boldsymbol{p}'^{\mathsf{T}} \left[(\boldsymbol{\omega}^{\mathrm{sc}_1};\, \boldsymbol{\omega}^{\mathrm{sl}}) \cdot \frac{\mathrm{d}^2(\boldsymbol{f}^{\mathrm{c}_1};\, \boldsymbol{f}^{\mathrm{l}})}{\mathrm{d}\boldsymbol{p}^2}\right] \boldsymbol{p}' > 0 \Leftrightarrow \boldsymbol{p}'^{\mathsf{T}} \left[(\boldsymbol{\omega}^{\mathrm{sc}_2};\, \boldsymbol{\omega}^{\mathrm{sl}}) \cdot \frac{\mathrm{d}^2(\boldsymbol{f}^{\mathrm{c}_2};\, \boldsymbol{f}^{\mathrm{l}})}{\mathrm{d}\boldsymbol{p}^2}\right] \boldsymbol{p}' > 0$$
$$\text{for any first-order flex } \boldsymbol{p}'.$$

(3) Different choices of diagonals for elementary length constraints do not change the prestress stability. In other words, suppose there are two choices of diagonals $\boldsymbol{f}^{\mathrm{l}_1}$ and $\boldsymbol{f}^{\mathrm{l}_2}$, there is a self-stress $\boldsymbol{\omega}^{\mathrm{sl}_1} \in \mathbb{R}^{n^{\mathrm{l}}}$ that can stabilize the rigid origami $G(\boldsymbol{p})$ with $\boldsymbol{\omega}^{\mathrm{sc}} \in \mathbb{R}^{n^{\mathrm{c}}}$ if and only if there is a self-stress $\boldsymbol{\omega}^{\mathrm{sl}_2} \in \mathbb{R}^{n^{\mathrm{l}}}$ that can stabilize $G(\boldsymbol{p})$ with $\boldsymbol{\omega}^{\mathrm{sc}} \in \mathbb{R}^{n^{\mathrm{c}}}$:

$$\boldsymbol{p}'^{\mathsf{T}} \left[(\boldsymbol{\omega}^{\mathrm{sc}};\, \boldsymbol{\omega}^{\mathrm{sl}_1}) \cdot \frac{\mathrm{d}^2(\boldsymbol{f}^{\mathrm{c}};\, \boldsymbol{f}^{\mathrm{l}_1})}{\mathrm{d}\boldsymbol{p}^2}\right] \boldsymbol{p}' > 0 \Leftrightarrow \boldsymbol{p}'^{\mathsf{T}} \left[(\boldsymbol{\omega}^{\mathrm{sc}};\, \boldsymbol{\omega}^{\mathrm{sl}_2}) \cdot \frac{\mathrm{d}^2(\boldsymbol{f}^{\mathrm{c}};\, \boldsymbol{f}^{\mathrm{l}_2})}{\mathrm{d}\boldsymbol{p}^2}\right] \boldsymbol{p}' > 0$$
$$\text{for any first-order flex } \boldsymbol{p}'.$$

Proof. As mentioned in the proof of Proposition 3.3, the motion of each panel is restricted to a rigid-body motion in a first-order flex. In addition, the transition of internal forces between different choices of coplanar and length constraints are explained in the proof of Proposition 4.1. From these properties, it can be said that the self-stress of the additional constraints within a single panel can be resolved locally by the self-stress corresponding to the elementary coplanar and length constraints, and the additional diagonals have no effect on the stability. Hence, we only need to prove that the quadratic form does not change for different choices of coplanar or length constraints within a single panel, since the procedure for a single panel can be repeated to all possible choices of constraints.

Suppose there is a pair of self-stresses $\boldsymbol{\omega}_1^{\mathrm{sc}_1}$ and $\boldsymbol{\omega}_1^{\mathrm{sl}}$ that can stabilize the rigid origami. Applying the transition of internal forces within a single panel, we have:

$$\begin{aligned}
(\boldsymbol{\omega}_1^{\mathrm{sc}_1}; \boldsymbol{\omega}_1^{\mathrm{sl}}; \mathbf{0}^{\mathrm{sca}'_1}) &= (\boldsymbol{\omega}_1^{\mathrm{sc}_1} + \boldsymbol{\omega}_2^{\mathrm{sc}_1}; \boldsymbol{\omega}_1^{\mathrm{sl}}; \boldsymbol{\omega}_1^{\mathrm{sca}'_1}) - (\boldsymbol{\omega}_2^{\mathrm{sc}_1}; \mathbf{0}^{\mathrm{sl}}; \boldsymbol{\omega}_1^{\mathrm{sca}'_1}) \\
&= (\boldsymbol{\omega}_1^{\mathrm{sc}_2}; \boldsymbol{\omega}_1^{\mathrm{sl}}; \boldsymbol{\omega}_1^{\mathrm{sca}'_2}) - (\boldsymbol{\omega}_2^{\mathrm{sc}_1}; \mathbf{0}^{\mathrm{sl}}; \boldsymbol{\omega}_1^{\mathrm{sca}'_1}) \\
&= (\boldsymbol{\omega}_1^{\mathrm{sc}_2} - \boldsymbol{\omega}_2^{\mathrm{sc}_2}; \boldsymbol{\omega}_1^{\mathrm{sl}}; \mathbf{0}^{\mathrm{sca}'_2}) + (\boldsymbol{\omega}_2^{\mathrm{sc}_2}; \mathbf{0}^{\mathrm{sl}}; \boldsymbol{\omega}_1^{\mathrm{sca}'_2}) - (\boldsymbol{\omega}_2^{\mathrm{sc}_1}; \mathbf{0}^{\mathrm{sl}}; \boldsymbol{\omega}_1^{\mathrm{sca}'_1}),
\end{aligned} \tag{40}$$

where $\boldsymbol{\omega}_1^{\mathrm{sca}'_1}$ and $\boldsymbol{\omega}_1^{\mathrm{sca}'_2}$ are the self-stresses of additional coplanar constraints **within the specified single panel**, whose components are **zero outside the specified panel**, corresponding to the different choices of elementary coplanar constraints $\boldsymbol{f}^{\mathrm{c}_1}$ and $\boldsymbol{f}^{\mathrm{c}_2}$, respectively. Then, $\boldsymbol{\omega}_2^{\mathrm{sc}_1}$ and $\boldsymbol{\omega}_2^{\mathrm{sc}_2}$ makes the second and third terms in the right-hand side of Eq. (40) self-stresses **with zero components outside the specified panel**, respectively. Since a self-stress within a single panel has no contribution to the stiffness, the quadratic form over the stress matrix does not change for different choices of coplanar constraints within a single panel. Exactly the same procedure can be used for different choices of length constraints, and the proof for the length constraints is omitted since it is straightforward from the proof for the coplanar constraints. □

5.2. Loaded case

In this subsection, we consider the case where the load $\boldsymbol{l}(\boldsymbol{p})$ that can be resolved and considered as the function of $\boldsymbol{p}$ is applied on a rigid origami. In this case, Definition 5.1 is modified as follows:

Definition 5.5. At a realization $\boldsymbol{p}$, a rigid origami $G(\boldsymbol{p})$ is stable under load $\boldsymbol{l}(\boldsymbol{p})$ if there is a positive definite matrix $\boldsymbol{E} \in \mathbb{R}^{(n^{\mathrm{c}}+n^{\mathrm{l}}+n^{\mathrm{ca}}+n^{\mathrm{la}})\times(n^{\mathrm{c}}+n^{\mathrm{l}}+n^{\mathrm{ca}}+n^{\mathrm{la}})}$ and a vector $\boldsymbol{\omega} \in \mathbb{R}^{n^{\mathrm{c}}+n^{\mathrm{l}}+n^{\mathrm{ca}}+n^{\mathrm{la}}}$ such that:

$$\frac{\mathrm{d}\boldsymbol{f}}{\mathrm{d}\boldsymbol{p}}^{\mathsf{T}}\boldsymbol{\omega} = \boldsymbol{l} \tag{41}$$

and

$$\boldsymbol{K} = \frac{\mathrm{d}\boldsymbol{f}}{\mathrm{d}\boldsymbol{p}}^{\mathsf{T}}\boldsymbol{E}\frac{\mathrm{d}\boldsymbol{f}}{\mathrm{d}\boldsymbol{p}} + \boldsymbol{\omega}\cdot\frac{\mathrm{d}^2\boldsymbol{f}}{\mathrm{d}\boldsymbol{p}^2} - \frac{\mathrm{d}\boldsymbol{l}}{\mathrm{d}\boldsymbol{p}} \tag{42}$$

is positive-definite

Proposition 5.6. (Stress test under a load) Restrict the perturbation at a realization $\boldsymbol{p}$ to the space of first-order flex; i.e., assume that the deformation only occurs in the direction of a first-order flex. Then, a rigid origami $G(\boldsymbol{p})$ is stable under the load $\boldsymbol{l}(\boldsymbol{p})$ if and only if there is a stress $\boldsymbol{\omega} \in \mathbb{R}^{n^{\mathrm{c}}+n^{\mathrm{l}}+n^{\mathrm{ca}}+n^{\mathrm{la}}}$ such that the stress matrix $\boldsymbol{\omega} \cdot \mathrm{d}^2\boldsymbol{f} \,/\, \mathrm{d}\boldsymbol{p}^2$ is positive definite over the space of first-order flex. Equivalently, a rigid origami is stable if and only if there is a stress $\boldsymbol{\omega}$ such that:

$$\bar{\boldsymbol{P}}'^{\mathsf{T}} \left[\boldsymbol{\omega} \cdot \frac{\mathrm{d}^2\boldsymbol{f}}{\mathrm{d}\boldsymbol{p}^2}\right] \bar{\boldsymbol{P}}' \in \mathbb{R}^{n^{\mathrm{f}} \times n^{\mathrm{f}}} \quad \text{is positive definite,} \tag{43}$$

where $\bar{\boldsymbol{P}}' \in \mathbb{R}^{3n^{\mathrm{v}} \times n^{\mathrm{f}}}$ is the matrix of the bases of first-order flex defined in Eq. (38).

Proof. From Proposition 5.2, a rigid origami $G(\boldsymbol{p})$ is stable under the load $\boldsymbol{l}(\boldsymbol{p})$ that can be resolved if and only if there is a stress $\boldsymbol{\omega} \in \mathbb{R}^{n^{\mathrm{c}}+n^{\mathrm{l}}+n^{\mathrm{ca}}+n^{\mathrm{la}}}$ which leads to a positive definite $\boldsymbol{\omega} \cdot \mathrm{d}^2\boldsymbol{f} \,/\, \mathrm{d}\boldsymbol{p}^2 - \mathrm{d}\boldsymbol{l} \,/\, \mathrm{d}\boldsymbol{p}$ over the space of first-order flex. Since a first-order flex $\boldsymbol{p}'$ is orthogonal to $\boldsymbol{l}$, the quadratic form $\boldsymbol{p}'^{\mathsf{T}}[\mathrm{d}\boldsymbol{l} \,/\, \mathrm{d}\boldsymbol{p}]\boldsymbol{p}' = 0$ for any $\boldsymbol{p}'$, and thus, $\boldsymbol{\omega} \cdot \mathrm{d}^2\boldsymbol{f} \,/\, \mathrm{d}\boldsymbol{p}^2 - \mathrm{d}\boldsymbol{l} \,/\, \mathrm{d}\boldsymbol{p}$ is positive definite. □

Remark 5.7. If the perturbation is considered in any direction, Proposition 5.6 no longer holds. However, in practice, the effect of the material term, which is the first term of the right-hand side of Eq. (42), is usually larger than that of the load term, which is the third term of the right-hand side of Eq. (42). Therefore, in many practical cases where the perturbation is not restricted, a rigid origami is stable if there is a stress $\boldsymbol{\omega}$ satisfying Eq. (43). In this case, $\bar{\boldsymbol{P}}'^{\mathsf{T}}[\boldsymbol{\omega} \cdot \mathrm{d}^2\boldsymbol{f} \,/\, \mathrm{d}\boldsymbol{p}^2]\bar{\boldsymbol{P}}'$ corresponds to the total stiffness matrix in the 'weakest' direction.

Proposition 5.8. (Invariance of stability under load) At a panel-wise generic realization, different choices of coplanar or length constraints have no effect on the stability under load which only depends on $\boldsymbol{p}$; i.e., (1) additional constraints do not change the stability, (2) different choices of vertices for elementary coplanar constraints do not change the stability, and (3) different choices of diagonals for elementary length constraints do not change the stability.

Proof. This proposition can be proved directly from the proof of Proposition 5.4. □

5.3. Hessian tensor

In this subsection, explicit calculation of the Hessian tensor $\mathrm{d}^2\boldsymbol{f} \,/\, \mathrm{d}\boldsymbol{p}^2$ is shown. First, the Hessian matrix of a coplanar constraint is shown. According to Eq. (3), nonzero components of the Hessian matrix of a coplanar constraint $f^{\mathrm{c}}(i,\, j,\, k,\, l)$ over $p_i,\ p_j,\ p_k,\ p_l$ for selected $i,\ j,\ k,\ l \in \mathbb{Z}^+$, $(i,\ j,\ k,\ l \leq$

n^{v}) on a hyper edge are:

$$\frac{\mathrm{d}^2 f^c(i,\, j,\, k,\, l)}{\mathrm{d}(p_i;\, p_j;\, p_k;\, p_l)^2} = \begin{bmatrix} 0 & [p_k - p_l]_\times & [p_l - p_j]_\times & [p_j - p_k]_\times \\ [p_l - p_k]_\times & 0 & [p_i - p_l]_\times & [p_k - p_i]_\times \\ [p_j - p_l]_\times & [p_l - p_i]_\times & 0 & [p_i - p_j]_\times \\ [p_k - p_j]_\times & [p_i - p_k]_\times & [p_j - p_i]_\times & 0 \end{bmatrix}, \tag{44}$$

where $[\cdot]_\times$ represents a cross product matrix generated from a vector, for example:

$$[p_i - p_j]_\times = \begin{bmatrix} 0 & p_{jz} - p_{iz} & p_{iy} - p_{jy} \\ p_{iz} - p_{jz} & 0 & p_{jx} - p_{ix} \\ p_{jy} - p_{iy} & p_{ix} - p_{jx} & 0 \end{bmatrix}, \tag{45}$$

where p_{ix}, p_{iy}, and p_{iz} are the x, y, and z-coordinates of vertex i ($i \in \mathbb{Z}^+,\ i \leq n^{\mathrm{v}}$). Also, from Eq. (4), nonzero components of the Hessian matrix of a length constraint $f^{\mathrm{l}}(i,\, j)$ between p_i and p_j are calculated for selected $i,\ j \in \mathbb{Z}^+,\ (i < j \leq n^{\mathrm{v}})$ as:

$$\frac{\partial^2 f^{\mathrm{l}}(i,\, j)}{\partial p_i^2} = \frac{\partial^2 f^{\mathrm{l}}(i,\, j)}{\partial p_j^2} = I,\ \frac{\partial^2 f^{\mathrm{l}}(i,\, j)}{\partial p_i \partial p_j} = \frac{\partial^2 f^{\mathrm{l}}(i,\, j)}{\partial p_j \partial p_i} = -I, \tag{46}$$

where I is the 3×3 identity matrix. Each component of the Hessian tensor $\mathrm{d}^2 f_k \,/\, \mathrm{d}\boldsymbol{p}^2 \in \mathbb{R}^{3n^{\mathrm{v}} \times 3n^{\mathrm{v}}}$ ($k \in \mathbb{Z}^+,\ k \leq n^{\mathrm{c}} + n^{\mathrm{l}} + n^{\mathrm{ca}} + n^{\mathrm{la}}$) is assembled from the second-order partial derivatives calculated as in Eqs. (44) and (46).

6. Second-order rigidity

In this section, we discuss the second-order rigidity and show its link with prestress stability. The second-order rigidity is an extension of first-order rigidity, derived from differentiating the constraints twice.

Definition 6.1. For a rigid origami $G(\boldsymbol{p})$, a second-order flex $(\boldsymbol{p}', \ \boldsymbol{p}'') \in (\mathbb{R}^{3n^{\mathrm{v}}}, \ \mathbb{R}^{3n^{\mathrm{v}}})$ is the solution of the equation with a slight abuse of notation for a product of a tensor and a vector below:

$$\begin{cases} \dfrac{\mathrm{d}\boldsymbol{f}}{\mathrm{d}\boldsymbol{p}}\boldsymbol{p}' = \boldsymbol{0} \\ \boldsymbol{p}'^{\mathsf{T}}\dfrac{\mathrm{d}^2\boldsymbol{f}}{\mathrm{d}\boldsymbol{p}^2}\boldsymbol{p}' + \dfrac{\mathrm{d}\boldsymbol{f}}{\mathrm{d}\boldsymbol{p}}\boldsymbol{p}'' = \boldsymbol{0} \end{cases} \quad (\boldsymbol{p}' \text{ is non-trivial}). \tag{47}$$

If there is no solution for a second-order flex, we say $G(\boldsymbol{p})$ is *second-order rigid*, otherwise *second-order flexible*.

Proposition 6.2. The following statements show the connection between the second-order rigidity and the self-stress or the prestress stability.

(1) A first-order flex $\boldsymbol{p}'$ can be extended to a second-order flex $\boldsymbol{p}''$ if and only if for all self-stress $\boldsymbol{\omega}^{\mathrm{s}}$,

$$\boldsymbol{p}'^{\mathsf{T}}\left[\boldsymbol{\omega}^{\mathrm{s}} \cdot \frac{\mathrm{d}^2\boldsymbol{f}}{\mathrm{d}\boldsymbol{p}^2}\right]\boldsymbol{p}' = 0. \tag{48}$$

(2) A rigid origami $G(\boldsymbol{p})$ is second-order rigid if and only if for any first-order

flex $\boldsymbol{p}'$ there is a self-stress $\boldsymbol{\omega}^{\mathrm{s}}(\boldsymbol{p}')$ such that:

$$\boldsymbol{p}'^{\mathsf{T}}\left[\boldsymbol{\omega}^{\mathrm{s}}(\boldsymbol{p}')\cdot\frac{\mathrm{d}^2\boldsymbol{f}}{\mathrm{d}\boldsymbol{p}^2}\right]\boldsymbol{p}'>0. \tag{49}$$

(3) If the rank of rigidity matrix for a given rigid origami $G(\boldsymbol{p})$ satisfies:

$$\operatorname{rank}\left(\frac{\mathrm{d}\boldsymbol{f}}{\mathrm{d}\boldsymbol{p}}\right)=3n^{\mathrm{v}}-7 \quad \text{or} \quad \operatorname{rank}\left(\frac{\mathrm{d}\boldsymbol{f}}{\mathrm{d}\boldsymbol{p}}\right)=n^{\mathrm{c}}+n^{\mathrm{l}}+n^{\mathrm{ca}}+n^{\mathrm{la}}-1, \tag{50}$$

then $G(\boldsymbol{p})$ is prestress stable if it is second-order rigid.

Proof. Statement (1): a first-order flex can be extended to a second-order flex if and only if there exists a solution for the linear system below:

$$\frac{\mathrm{d}\boldsymbol{f}}{\mathrm{d}\boldsymbol{p}}\boldsymbol{p}''=-\boldsymbol{p}'^{\mathsf{T}}\frac{\mathrm{d}^2\boldsymbol{f}}{\mathrm{d}\boldsymbol{p}^2}\boldsymbol{p}', \tag{51}$$

which means the right hand side of the above equation should lie in the column space of the rigidity matrix, hence is orthogonal to any self stress $\boldsymbol{\omega}^{\mathrm{s}}$ in the left null space.

Statement (2): from the inverse negative of statement (1), a rigid origami is second-order rigid if and only if, for any non-trivial first order-flex $\boldsymbol{p}'$, there is a self-stress $\boldsymbol{\omega}^{\mathrm{s}}(\boldsymbol{p}')$ such that:

$$\boldsymbol{p}'^{\mathsf{T}}\left[\boldsymbol{\omega}^{\mathrm{s}}(\boldsymbol{p}')\cdot\frac{\mathrm{d}^2\boldsymbol{f}}{\mathrm{d}\boldsymbol{p}^2}\right]\boldsymbol{p}'\neq 0. \tag{52}$$

Either this quadratic form is positive, or can be made positive by replacing

$\boldsymbol{\omega}^{\mathrm{s}}$ with $-\boldsymbol{\omega}^{\mathrm{s}}$.

Statement (3): from statement (2), for any first-order flex $\boldsymbol{p}'$ there is a self-stress $\boldsymbol{\omega}^{\mathrm{s}}(\boldsymbol{p}')$ such that:

$$\boldsymbol{p}'^{\mathsf{T}} \left[\boldsymbol{\omega}^{\mathrm{s}}(\boldsymbol{p}') \cdot \frac{\mathrm{d}^2 \boldsymbol{f}}{\mathrm{d}\boldsymbol{p}^2} \right] \boldsymbol{p}' > 0. \tag{53}$$

When the dimension of the space of first-order flex is 1, clearly the self-stress for a basis of the first-order flex stabilizes this rigid origami.

Next, when the dimension of the space of self-stress is 1, denote a basis of the space of self-stress as $\bar{\boldsymbol{\omega}}_1^{\mathrm{s}}$. If this rigid origami is not prestress stable, there exists a first-order flex $\boldsymbol{p}'$ such that for all choice of γ,

$$\boldsymbol{p}'^{\mathsf{T}} \left[\gamma \bar{\boldsymbol{\omega}}_1^{\mathrm{s}} \cdot \frac{\mathrm{d}^2 \boldsymbol{f}}{\mathrm{d}\boldsymbol{p}^2} \right] \boldsymbol{p}' = 0, \tag{54}$$

which contradicts with the condition of second-order rigidity. $\square$

Corollary 6.3. From Proposition 6.2, a rigid origami $G(\boldsymbol{p})$ is second-order rigid if and only if there is no common solution for all the quadratic forms below:

$$\boldsymbol{x}^{\mathsf{T}} \left(\bar{\boldsymbol{P}}'^{\mathsf{T}} \left[\bar{\boldsymbol{\omega}}_i^{\mathrm{s}} \cdot \frac{\mathrm{d}^2 \boldsymbol{f}}{\mathrm{d}\boldsymbol{p}^2} \right] \bar{\boldsymbol{P}}' \right) \boldsymbol{x} = 0. \tag{55}$$

It can be seen from Proposition 6.2 that, prestress stability requires a single self-stress such that the quadratic form is positive for every first-order flex, while the second-order rigidity requires a “suitable” self-stress for every first-order flex such that the quadratic form is positive. Physically, such a self-stress “blocks” a possible second-order flex for a given first-order flex.

Proposition 6.4. (Invariance of the second-order rigidity) Different choices of coplanar or length constraints have no effect on the second-order rigidity at a panel-wise generic realization:

(1) Additional constraints do not change the space of second-order flex. In other words, there is a self-stress $\boldsymbol{\omega}^{\mathrm{s}} \in \mathbb{R}^{n^{\mathrm{c}}+n^{\mathrm{l}}+n^{\mathrm{ca}}+n^{\mathrm{la}}}$ that can block a first-order flex $\boldsymbol{p}' \in \mathbb{R}^{3n^{\mathrm{v}}}$ if and only if there is a pair of self-stresses $\boldsymbol{\omega}^{\mathrm{sc}} \in \mathbb{R}^{n^{\mathrm{c}}}$ and $\boldsymbol{\omega}^{\mathrm{sl}} \in \mathbb{R}^{n^{\mathrm{l}}}$ that can block $\boldsymbol{p}'$:

$$\boldsymbol{p}'^{\mathsf{T}} \frac{\mathrm{d}^2 \boldsymbol{f}}{\mathrm{d}\boldsymbol{p}^2} \boldsymbol{p}' + \frac{\mathrm{d}\boldsymbol{f}}{\mathrm{d}\boldsymbol{p}} \boldsymbol{p}'' = \mathbf{0} \Leftrightarrow \boldsymbol{p}'^{\mathsf{T}} \frac{\mathrm{d}^2 (\boldsymbol{f}^{\mathrm{c}};\, \boldsymbol{f}^{\mathrm{l}})}{\mathrm{d}\boldsymbol{p}^2} \boldsymbol{p}' + \frac{\mathrm{d}(\boldsymbol{f}^{\mathrm{c}};\, \boldsymbol{f}^{\mathrm{l}})}{\mathrm{d}\boldsymbol{p}} \boldsymbol{p}'' = \mathbf{0},$$
$$\boldsymbol{p}'^{\mathsf{T}} \left[\boldsymbol{\omega}^{\mathrm{s}} \cdot \frac{\mathrm{d}^2 \boldsymbol{f}}{\mathrm{d}\boldsymbol{p}^2} \right] \boldsymbol{p}' > 0 \Leftrightarrow \boldsymbol{p}'^{\mathsf{T}} \left[(\boldsymbol{\omega}^{\mathrm{sc}};\, \boldsymbol{\omega}^{\mathrm{sl}}) \cdot \frac{\mathrm{d}^2 (\boldsymbol{f}^{\mathrm{c}};\, \boldsymbol{f}^{\mathrm{l}})}{\mathrm{d}\boldsymbol{p}^2} \right] \boldsymbol{p}' > 0.$$

(2) Different choices of vertices for coplanar constraints do not change the space of second-order flex. In other words, suppose there are two choices of coplanar constraints $\boldsymbol{f}^{\mathrm{c}_1}$ and $\boldsymbol{f}^{\mathrm{c}_2}$, there is a self-stress $\boldsymbol{\omega}^{\mathrm{sc}_1} \in \mathbb{R}^{n^{\mathrm{c}}}$ that can block a first-order flex $\boldsymbol{p}' \in \mathbb{R}^{3n^{\mathrm{v}}}$ with $\boldsymbol{\omega}^{\mathrm{sl}} \in \mathbb{R}^{n^{\mathrm{l}}}$ if and only if there is a self-stress $\boldsymbol{\omega}^{\mathrm{sc}_1} \in \mathbb{R}^{n^{\mathrm{c}}}$ that can block $\boldsymbol{p}'$ with $\boldsymbol{\omega}^{\mathrm{sl}}$:

$$\boldsymbol{p}'^{\mathsf{T}} \frac{\mathrm{d}^2 (\boldsymbol{f}^{\mathrm{c}_1};\, \boldsymbol{f}^{\mathrm{l}})}{\mathrm{d}\boldsymbol{p}^2} \boldsymbol{p}' + \frac{\mathrm{d}(\boldsymbol{f}^{\mathrm{c}_1};\, \boldsymbol{f}^{\mathrm{l}})}{\mathrm{d}\boldsymbol{p}} \boldsymbol{p}'' = \mathbf{0} \Leftrightarrow \boldsymbol{p}'^{\mathsf{T}} \frac{\mathrm{d}^2 (\boldsymbol{f}^{\mathrm{c}_2};\, \boldsymbol{f}^{\mathrm{l}})}{\mathrm{d}\boldsymbol{p}^2} \boldsymbol{p}' + \frac{\mathrm{d}(\boldsymbol{f}^{\mathrm{c}_2},\, \boldsymbol{f}^{\mathrm{l}})}{\mathrm{d}\boldsymbol{p}} \boldsymbol{p}'' = \mathbf{0},$$
$$\boldsymbol{p}'^{\mathsf{T}} \left[(\boldsymbol{\omega}^{\mathrm{sc}_1};\, \boldsymbol{\omega}^{\mathrm{sl}}) \cdot \frac{\mathrm{d}^2 (\boldsymbol{f}^{\mathrm{c}_2};\, \boldsymbol{f}^{\mathrm{l}})}{\mathrm{d}\boldsymbol{p}^2} \right] \boldsymbol{p}' > 0 \Leftrightarrow \boldsymbol{p}'^{\mathsf{T}} \left[(\boldsymbol{\omega}^{\mathrm{sc}_2};\, \boldsymbol{\omega}^{\mathrm{sl}}) \cdot \frac{\mathrm{d}^2 (\boldsymbol{f}^{\mathrm{c}_2};\, \boldsymbol{f}^{\mathrm{l}})}{\mathrm{d}\boldsymbol{p}^2} \right] \boldsymbol{p}' > 0.$$

(3) Different choices of diagonals for generically proper length constraints do not change the space of second-order flex. In other words, suppose there

are two choices of diagonals $\boldsymbol{f}^{\mathrm{l}_1}$ and $\boldsymbol{f}^{\mathrm{l}_2}$, there is a self-stress $\boldsymbol{\omega}^{\mathrm{sl}_1} \in \mathbb{R}^{n^{\mathrm{l}}}$ that can block a first-order flex $\boldsymbol{p}' \in \mathbb{R}^{3n^{\mathrm{v}}}$ with $\boldsymbol{\omega}^{\mathrm{sc}} \in \mathbb{R}^{n^{\mathrm{c}}}$ if and only if there is a self-stress $\boldsymbol{\omega}^{\mathrm{sl}_1} \in \mathbb{R}^{n^{\mathrm{l}}}$ that can block $\boldsymbol{p}'$ with $\boldsymbol{\omega}^{\mathrm{sc}}$:

$$
\begin{aligned}
\boldsymbol{p}'^{\mathsf{T}} \frac{\mathrm{d}^2(\boldsymbol{f}^{\mathrm{c}};\, \boldsymbol{f}^{\mathrm{l}_1})}{\mathrm{d}\boldsymbol{p}^2}\boldsymbol{p}' + \frac{\mathrm{d}(\boldsymbol{f}^{\mathrm{c}};\, \boldsymbol{f}^{\mathrm{l}_1})}{\mathrm{d}\boldsymbol{p}}\boldsymbol{p}'' = \boldsymbol{0} \Leftrightarrow \boldsymbol{p}'^{\mathsf{T}} \frac{\mathrm{d}^2(\boldsymbol{f}^{\mathrm{c}};\, \boldsymbol{f}^{\mathrm{l}_2})}{\mathrm{d}\boldsymbol{p}^2}\boldsymbol{p}' + \frac{\mathrm{d}(\boldsymbol{f}^{\mathrm{c}};\, \boldsymbol{f}^{\mathrm{l}_2})}{\mathrm{d}\boldsymbol{p}}\boldsymbol{p}'' = \boldsymbol{0},\\
\boldsymbol{p}'^{\mathsf{T}} \left[(\boldsymbol{\omega}^{\mathrm{sc}};\, \boldsymbol{\omega}^{\mathrm{sl}_1}) \cdot \frac{\mathrm{d}^2(\boldsymbol{f}^{\mathrm{c}};\, \boldsymbol{f}^{\mathrm{l}_1})}{\mathrm{d}\boldsymbol{p}^2}\right]\boldsymbol{p}' > 0 \Leftrightarrow \boldsymbol{p}'^{\mathsf{T}} \left[(\boldsymbol{\omega}^{\mathrm{sc}};\, \boldsymbol{\omega}^{\mathrm{sl}_2}) \cdot \frac{\mathrm{d}^2(\boldsymbol{f}^{\mathrm{c}},\, \boldsymbol{f}^{\mathrm{l}_2})}{\mathrm{d}\boldsymbol{p}^2}\right]\boldsymbol{p}' > 0.
\end{aligned}
$$

Proof. The proof has been included in the proof of Proposition 5.4. □

7. Displacement boundary condition

This section introduces the procedure for incorporating the boundary conditions assigned to the vertex displacements. Let $n^{\mathrm{b}} \in \mathbb{Z}^+$ denote the number of displacement boundary conditions, and the corresponding constraints on $\boldsymbol{p}$ are written by using the n^{b} column vector $\boldsymbol{f}^{\mathrm{b}}$ as:

$$\boldsymbol{f}^{\mathrm{b}}(\boldsymbol{p}) = \boldsymbol{0}. \tag{56}$$

Then, the rigidity of a rigid origami under the boundary constraints is investigated by adding $\boldsymbol{f}^{\mathrm{b}}$ to $\boldsymbol{f}$ as $\boldsymbol{f} = (\boldsymbol{f}^{\mathrm{c}};\, \boldsymbol{f}^{\mathrm{l}};\, \boldsymbol{f}^{\mathrm{ca}};\, \boldsymbol{f}^{\mathrm{la}};\, \boldsymbol{f}^{\mathrm{b}})$. The definitions of the first-order flex, the second-order flex, and most of the rigidity in the previous sections remain unchanged by this extension of $\boldsymbol{f}$ except for the first-order rigidity.

Definition 7.1. A rigid origami $G(\boldsymbol{p})$ is *first-order rigid* if it has no first-

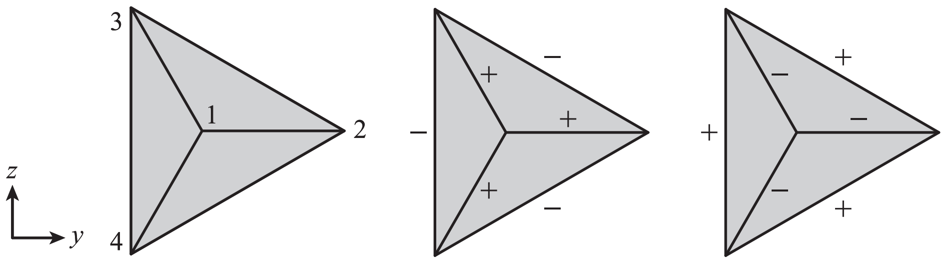

(a) (b) (c)

Figure 5: A planar rigid origami with a single degree-3 interior vertex which is first-order flexible and prestress stable. Different self-stress affects the stability. (a) Labelling of vertices, (b) Distribution of self-stress which achieves a **stable** equilibrium state, (c) Distribution of self-stress which achieves an **unstable** equilibrium state ($+$ and $-$ symbols next to the edges represent positive and negative self-stresses, respectively, corresponding to tension and compression axial force (or force density) along edges of the rigid origami)

order flex or only trivial first-order flex. Note that especially when $\boldsymbol{f}^{\mathrm{b}}$ restricts all the trivial first-order flexes, a rigid origami $G(\boldsymbol{p})$ is first-order rigid if $\mathrm{rank}(\mathrm{d}(\boldsymbol{f}^{\mathrm{c}};\, \boldsymbol{f}^{\mathrm{l}};\, \boldsymbol{f}^{\mathrm{ca}};\, \boldsymbol{f}^{\mathrm{la}};\, \boldsymbol{f}^{\mathrm{b}}) \,/\, \mathrm{d}\boldsymbol{p}) = 3n^{\mathrm{v}}$.

It is also clear from the proofs that the invariance of the rigidity and stability with respect to the choices of the constraints is guaranteed even when the boundary conditions are assigned.

The standard procedure in structural engineering for incorporating a simple displacement boundary condition p_{ix} = const., p_{iy} = const., or p_{iz} = const. $(i \in \mathbb{Z}^{+},\ i \leq n^{\mathrm{v}})$ can also be employed; i.e., the columns of the rigidity matrix and the components of the Hessian tensor corresponding the constrained coordinates are removed and the size of the vectors representing the first-order and second-order flexes are reduced if they exist. In the following examples, this approach is used.

Example 2. Consider a planar rigid origami with a single degree-3 interior vertex in Fig. 5. The coordinates of vertices are given as:

$$\begin{aligned} &\text{vertex 1: } (0,\,0,\,0), && \text{vertex 2: } (1,\,0,\,0), \\ &\text{vertex 3: } \left(-\frac{1}{2},\,\frac{\sqrt{3}}{2},\,0\right), && \text{vertex 4: } \left(-\frac{1}{2},\,-\frac{\sqrt{3}}{2},\,0\right). \end{aligned}$$

To constrain the overall rigid-body motion, the $y,\ z$ coordinates of vertex 2, the z coordinate of vertex 3 and the $x,\ y,\ z$ coordinates of vertex 4 are fixed. Note that this is one of the possible boundary conditions for constraining the rigid-body motion.

The rigidity matrix for this planar degree-3 vertex example under above boundary conditions has the size of 6×6, and its components are provided in Appendix A.1. The rank of the rigidity matrix is 5, and the first-order flex, self-stress, load that can be resolved, and internal force corresponding to load can be written as follows:

$$\boldsymbol{p}' = a \begin{pmatrix} 0 \\ 0 \\ 1 \\ 0 \\ 0 \\ 0 \end{pmatrix}, \ \boldsymbol{\omega}^{\mathrm{s}} = b \begin{pmatrix} 3 \\ 3 \\ 3 \\ -1 \\ -1 \\ -1 \end{pmatrix}, \ \boldsymbol{l} = \begin{pmatrix} c_1 \\ c_2 \\ 0 \\ c_3 \\ c_4 \\ c_5 \end{pmatrix},$$

$$\boldsymbol{\omega} = \begin{pmatrix} 3b - c_1 + \frac{1}{3}c_2 + c_4 + c_5 \\ 3b + c_4 + c_5 \\ 3b + \frac{2}{3}c_2 + c_4 + c_5 \\ -b - c_4 - \frac{1}{3}c_5 \\ -b + \frac{2}{3}c_1 - \frac{2}{9}c_2 + \frac{2}{3}c_3 + \frac{1}{3}c_4 - \frac{1}{3}c_5 \\ -b_1 \end{pmatrix},$$

$$a, \ b, \ c_1, \ c_2, \ c_3, \ c_4, \ c_5 \in \mathbb{R},$$

where the components of the self-stress and the internal force correspond to the length constraints between vertices (1, 2), (1, 3), (1, 4), (2, 3), (2, 4), (3, 4), from top to bottom. The physical meaning is clear: the only non-trivial first-order flex is a out-of-plane motion at vertex 1 when the above mentioned boundary condition is assigned. The self-stress is cyclically symmetric to vertex 1.

To analyze the prestress stability and the stability under the load that can be resolved, Propositions 5.2 and 5.6 are applied to the rigid origami in Fig. 5. The stress matrices under the given displacement boundary conditions are calculated in Appendix A.1, and the quadratic forms over a first-order flex are:

$$\boldsymbol{p}'^{\mathsf{T}}\left[\boldsymbol{\omega}^{\mathrm{s}}\cdot\frac{\mathrm{d}^2\boldsymbol{f}}{\mathrm{d}\boldsymbol{p}^2}\right]\boldsymbol{p}' = 9a^2 b,$$
$$\boldsymbol{p}'^{\mathsf{T}}\left[\boldsymbol{\omega}\cdot\frac{\mathrm{d}^2\boldsymbol{f}}{\mathrm{d}\boldsymbol{p}^2}\right]\boldsymbol{p}' = (9b - c_1 + c_2 + 3c_4 + 3c_5)\, a^2.$$

If there is no load, the rigid origami is stable when $b > 0$ (Fig. 5(b)), while it is unstable when $b < 0$ (Fig. 5(c)). This stress distribution in the stable equilibrium state – the interior edges are in tension and the external edges are in compression, is well-known in the study of tensegrity structures. On the other hand, if external load is applied, the rigid origami is stable when $9b-c_1+c_2+3c_4+3c_5 > 0$, where the positive $-c_1+c_2+3c_4+3c_5 > 0$ leads to the above stable stress distribution. It should be noted that the same example is investigated using a rotational hinge model (folding angle description) in Ref. [1], and the results for the stress tests are different; the quadric forms in the unloaded case and loaded case are identical in the rotational hinge model while they are different in the panel-point model. This difference is attributed to the range of loads that can be considered in each model. The panel-point model can consider loads that tensile/compress the entire rigid origami in-plane, as in this example, whereas the rotational hinge model does not.

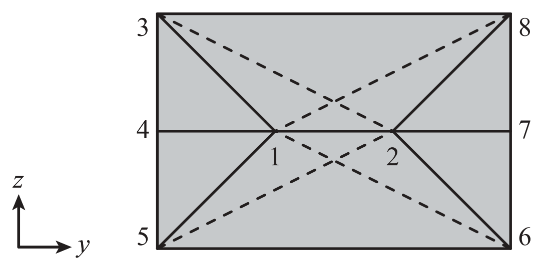

Figure 6: A rigid origami with two degree-4 interior vertices with 8 vertices, 13 panel boundary lines (solid line), and 4 diagonals (dotted line).

Example 3. A rigid origami with two interior degree-4 vertices shown in Fig. 6 is considered, which has 8 vertices, 7 crease lines, 6 boundary lines, and 4 diagonals. It is second-order flexible at the planar and three-dimensional realization with specified boundary conditions, and it is second-order rigid by adding an extra boundary condition. The hyper edges of the underlying graph of this rigid origami are listed below.

$$\{1,\,3,\,4\},\ \{1,\,4,\,5\},\ \{2,\,6,\,7\},\ \{2,\,7,\,8\},$$
$$\{1,\,2,\,8,\,3\},\ \{1,\,5,\,6,\,2\}.$$

Here, planar and three-dimensional realizations are considered, and the x and y-coordinates of vertices are listed as follows:

vertex 1: $(-1,\,0)$, vertex 2: $(1,\,0)$, vertex 3: $(-3,\,2)$, vertex 4: $(-3,\,0)$,

vertex 5: $(-3,\,-2)$, vertex 6: $(3,\,-2)$, vertex 7: $(3,\,0)$, vertex 8: $(3,\,2)$.

At the planar realization, the z-coordinates of all the vertices are 0 while at the three-dimensional realization, the z-coordinates of vertices 1, 2 are 2 and those of vertices 3 – 8 are 0.

First, to constrain the rigid-body motion of the rigid origami, the x and z-coordinates of vertices 2, 4 and the y and z-coordinates of vertex 6 are fixed. Then, the size of rigidity matrix is 19×18 consisting of 2 coplanar constraints and 17 length constraints, and at the planar realization, $\operatorname{rank}(\mathrm{d}\boldsymbol{f} \,/\, \mathrm{d}\boldsymbol{p}) = 15$. Therefore, the dimensions of the non-trivial first-order flex and the self-stress are $n^{\mathrm{f}} = 3$ and $n^{\mathrm{s}} = 4$, respectively. A first-order flex and a self-stress are provided in Appendix A.2 with the parameters $a_1,\ a_2,\ a_3 \in \mathbb{R}$ and $b_1,\ b_2,\ b_3,\ b_4 \in \mathbb{R}$, respectively. The matrices $\bar{\boldsymbol{P}}'^{\mathsf{T}}[\bar{\boldsymbol{\omega}}_i^{\mathrm{s}} \cdot \mathrm{d}^2\boldsymbol{f} \,/\, \mathrm{d}\boldsymbol{p}^2]\bar{\boldsymbol{P}}'$ $(i = 1,\, 2,\, 3,\, 4)$ are also shown in Appendix A.2 for the investigation of the second-order rigidity. At the unloaded planar realization, Eq. (55) for all $i = 1,\, 2,\, 3,\, 4$ are summarized into the following equations:

$$\begin{cases} a_1^2 - 10a_1a_2 + 7a_2^2 + a_3^2 = 0, \\ 5a_1^2 - 14a_1a_2 + 8a_2^2 = 0. \end{cases}$$

The common solutions for the above equations are:

$$(a_1,\, a_2,\, a_3) = (2a,\, a,\, \pm 3a),\ (4a,\, 5a,\, \pm 3a) \quad \text{for any } a \in \mathbb{R}.$$

Hence, this planar rigid origami is second-order flexible, and the first-order flex in the direction described in the above equation can be extended to a second-order flex.

On the other hand, at the three-dimensional realization, $\operatorname{rank}(\mathrm{d}\boldsymbol{f} \,/\, \mathrm{d}\boldsymbol{p}) =$

16, and the dimensions of the non-trivial first-order flex and the self-stress are $n^{\mathrm{f}} = 2$ and $n^{\mathrm{s}} = 3$, respectively. At the unloaded three-dimensional realization, Eq. (55) for all the bases of self-stress are summarized into the following equation:

$$a_1^2 - a_2^2 = 0.$$

The solutions for the above equation are:

$$(a_1,\, a_2) = (a,\, \pm a) \quad \text{for any } a \in \mathbb{R}.$$

Hence, this three-dimensional rigid origami is second-order flexible, and the first-order flex in the direction described in the above equation can be extended to a second-order flex.

Next, a further boundary condition is added to the three-dimensional rigid origami. The extra boundary condition is assigned so that the z coordinate of vertex 1 is fixed. The size of the rigidity matrix is reduced to 19×17, and $\operatorname{rank}\left(\mathrm{d}\boldsymbol{f} \,/\, \mathrm{d}\boldsymbol{p}\right) = 16$. Therefore, the dimensions of the non-trivial first-order flex and the self-stress are $n^{\mathrm{f}} = 1$ and $n^{\mathrm{s}} = 3$, respectively. In the unloaded case, the quadratic form over a first-order flex is:

$$\boldsymbol{p}'^{\top} \left[\boldsymbol{\omega}^{\mathrm{s}} \cdot \frac{\mathrm{d}^2 \boldsymbol{f}}{\mathrm{d}\boldsymbol{p}^2}\right] \boldsymbol{p}' = 4\,(b_2 - b_3)\, a^2.$$

Hence, this rigid origami is second-order rigid and prestress stable when $b_2 > b_3$.

8. Conclusions

This article has introduced a methodology for analyzing the rigidity and flexibility of a rigid origami, which is described in terms of the Euclidean coordinates of its vertices. The efficiency of this methodology has been validated through a series of examples, including the cases with and without displacement boundary conditions. Furthermore, we have demonstrated that the key quantities in rigidity analysis remain invariant regardless of the choice of coplanar and length constraints. The only quantity that changes due to the different choices of constraints is the internal force distribution, and the transition of the distribution is also shown. While this article has primarily focused on rigidity analysis, the panel-point model can also be applied to analysis of the higher-order and finite flexibility of rigid origami, given that the constraints are formulated in the polynomial forms. The panel-point model captures the kinematics of rigid origami more completely than the truss model by introducing coplanar constraints and is more directly applicable to CAD and numerical analysis. Furthermore, it covers a wide range of structures and mechanisms consisting of flat panels connected by hinges and pins, not limited to rigid origami, due to its formulation of constraints.

Acknowledgements

Kentaro Hayakawa was partly supported by JSPS KAKENHI Grant Number JP20J21650. Zeyuan He would like to thank the funding support from the MathWorks Ltd. We also would like to acknowledge Prof. Makoto Ohsaki at Kyoto University for his assistance in launching this project.

Appendix A. Detailed calculations of derivatives

Appendix A.1. Calculations for Example 2

The rigidity matrix for Example 2 under the given boundary conditions is:

$$\frac{\mathrm{d}\boldsymbol{f}}{\mathrm{d}\boldsymbol{p}} = \begin{bmatrix} -1 & 0 & 0 & 1 & 0 & 0 \\ \frac{1}{2} & -\frac{\sqrt{3}}{2} & 0 & 0 & -\frac{1}{2} & \frac{\sqrt{3}}{2} \\ \frac{1}{2} & \frac{\sqrt{3}}{2} & 0 & 0 & 0 & 0 \\ 0 & 0 & 0 & \frac{3}{2} & -\frac{3}{2} & \frac{\sqrt{3}}{2} \\ 0 & 0 & 0 & \frac{3}{2} & 0 & 0 \\ 0 & 0 & 0 & 0 & 0 & \sqrt{3} \end{bmatrix}.$$

The rows are for length constraints between vertices (1, 2), (1, 3), (1, 4), (2, 3), (2, 4), (3, 4), from top to bottom.

The Hessian matrix for each length constraint under the given fixed boundary condition is calculated as:

$$
\frac{\mathrm{d}^2 f^1(1,\ 2)}{\mathrm{d}\boldsymbol{p}^2} = \begin{bmatrix} 1 & 0 & 0 & -1 & 0 & 0 \\ 0 & 1 & 0 & 0 & 0 & 0 \\ 0 & 0 & 1 & 0 & 0 & 0 \\ -1 & 0 & 0 & 1 & 0 & 0 \\ 0 & 0 & 0 & 0 & 0 & 0 \\ 0 & 0 & 0 & 0 & 0 & 0 \end{bmatrix}, \quad \frac{\mathrm{d}^2 f^1(1,\ 3)}{\mathrm{d}\boldsymbol{p}^2} = \begin{bmatrix} 1 & 0 & 0 & 0 & -1 & 0 \\ 0 & 1 & 0 & 0 & 0 & -1 \\ 0 & 0 & 1 & 0 & 0 & 0 \\ 0 & 0 & 0 & 0 & 0 & 0 \\ -1 & 0 & 0 & 0 & 1 & 0 \\ 0 & -1 & 0 & 0 & 0 & 1 \end{bmatrix},
$$

$$
\frac{\mathrm{d}^2 f^1(1,\ 4)}{\mathrm{d}\boldsymbol{p}^2} = \begin{bmatrix} 1 & 0 & 0 & 0 & 0 & 0 \\ 0 & 1 & 0 & 0 & 0 & 0 \\ 0 & 0 & 1 & 0 & 0 & 0 \\ 0 & 0 & 0 & 0 & 0 & 0 \\ 0 & 0 & 0 & 0 & 0 & 0 \\ 0 & 0 & 0 & 0 & 0 & 0 \end{bmatrix}, \quad \frac{\mathrm{d}^2 f^1(2,\ 3)}{\mathrm{d}\boldsymbol{p}^2} = \begin{bmatrix} 0 & 0 & 0 & 0 & 0 & 0 \\ 0 & 0 & 0 & 0 & 0 & 0 \\ 0 & 0 & 0 & 0 & 0 & 0 \\ 0 & 0 & 0 & 1 & -1 & 0 \\ 0 & 0 & 0 & -1 & 1 & 0 \\ 0 & 0 & 0 & 0 & 0 & 1 \end{bmatrix},
$$

$$
\frac{\mathrm{d}^2 f^1(2,\ 4)}{\mathrm{d}\boldsymbol{p}^2} = \begin{bmatrix} 0 & 0 & 0 & 0 & 0 & 0 \\ 0 & 0 & 0 & 0 & 0 & 0 \\ 0 & 0 & 0 & 0 & 0 & 0 \\ 0 & 0 & 0 & 1 & 0 & 0 \\ 0 & 0 & 0 & 0 & 0 & 0 \\ 0 & 0 & 0 & 0 & 0 & 0 \end{bmatrix}, \quad \frac{\mathrm{d}^2 f^1(3,\ 4)}{\mathrm{d}\boldsymbol{p}^2} = \begin{bmatrix} 0 & 0 & 0 & 0 & 0 & 0 \\ 0 & 0 & 0 & 0 & 0 & 0 \\ 0 & 0 & 0 & 0 & 0 & 0 \\ 0 & 0 & 0 & 0 & 0 & 0 \\ 0 & 0 & 0 & 0 & 1 & 0 \\ 0 & 0 & 0 & 0 & 0 & 1 \end{bmatrix}.
$$

Hence, the stress matrix for the self-stress is:

$$\boldsymbol{\omega}^{\mathrm{s}} \cdot \frac{\mathrm{d}^2 \boldsymbol{f}}{\mathrm{d}\boldsymbol{p}^2} = b \begin{bmatrix} 9 & 0 & 0 & -3 & -3 & 0 \\ 0 & 9 & 0 & 0 & 0 & -3 \\ 0 & 0 & 9 & 0 & 0 & 0 \\ -3 & 0 & 0 & 1 & 1 & 0 \\ -3 & 0 & 0 & 1 & 1 & 0 \\ 0 & -3 & 0 & 0 & 0 & 1 \end{bmatrix},$$

and the stress matrix for the stress under the load that can be resolved is:

$$
\begin{aligned}
\boldsymbol{\omega}\cdot\frac{\mathrm{d}^2\boldsymbol{f}}{\mathrm{d}\boldsymbol{p}^2} =& b\begin{bmatrix} 9 & 0 & 0 & -3 & -3 & 0 \\ 0 & 9 & 0 & 0 & 0 & -3 \\ 0 & 0 & 9 & 0 & 0 & 0 \\ -3 & 0 & 0 & 1 & 1 & 0 \\ -3 & 0 & 0 & 1 & 1 & 0 \\ 0 & -3 & 0 & 0 & 0 & 1 \end{bmatrix} + c_1\begin{bmatrix} -1 & 0 & 0 & 1 & 0 & 0 \\ 0 & -1 & 0 & 0 & 0 & 0 \\ 0 & 0 & -1 & 0 & 0 & 0 \\ 1 & 0 & 0 & -\frac{1}{3} & 0 & 0 \\ 0 & 0 & 0 & 0 & 0 & 0 \\ 0 & 0 & 0 & 0 & 0 & 0 \end{bmatrix} \\
& + c_2\begin{bmatrix} 1 & 0 & 0 & -\frac{1}{3} & 0 & 0 \\ 0 & 1 & 0 & 0 & 0 & 0 \\ 0 & 0 & 1 & 0 & 0 & 0 \\ -\frac{1}{3} & 0 & 0 & \frac{1}{9} & 0 & 0 \\ 0 & 0 & 0 & 0 & 0 & 0 \\ 0 & 0 & 0 & 0 & 0 & 0 \end{bmatrix} + c_3\begin{bmatrix} 0 & 0 & 0 & 0 & 0 & 0 \\ 0 & 0 & 0 & 0 & 0 & 0 \\ 0 & 0 & 0 & 0 & 0 & 0 \\ 0 & 0 & 0 & \frac{2}{3} & 0 & 0 \\ 0 & 0 & 0 & 0 & 0 & 0 \\ 0 & 0 & 0 & 0 & 0 & 0 \end{bmatrix} \\
& + c_4\begin{bmatrix} 3 & 0 & 0 & -1 & -1 & 0 \\ 0 & 3 & 0 & 0 & 0 & -1 \\ 0 & 0 & 3 & 0 & 0 & 0 \\ -1 & 0 & 0 & \frac{1}{3} & 1 & 0 \\ -1 & 0 & 0 & 1 & 0 & 0 \\ 0 & -1 & 0 & 0 & 0 & 0 \end{bmatrix} + c_5\begin{bmatrix} 3 & 0 & 0 & -1 & -1 & 0 \\ 0 & 3 & 0 & 0 & 0 & -1 \\ 0 & 0 & 3 & 0 & 0 & 0 \\ -1 & 0 & 0 & \frac{1}{3} & \frac{1}{3} & 0 \\ -1 & 0 & 0 & \frac{1}{3} & \frac{2}{3} & 0 \\ 0 & -1 & 0 & 0 & 0 & \frac{2}{3} \end{bmatrix}.
\end{aligned}
$$

Appendix A.2. Calculations for Example 3

In this section, Example 3 is considered. When the x and z-coordinates of vertices 2, 4 and the y and z-coordinates of vertex 6 are fixed, the size of rigidity matrix is 19×18 consisting of 2 coplanar constraints and 17 length constraints where the last 17 rows are for length constraints between vertices (1, 2), (1, 3), (1, 4), (1, 5), (2, 6), (2, 7), (2, 8), (3, 4), (4, 5), (5, 6), (6, 7), (7, 8), (3, 8), (1, 8), (1, 6), (2, 3), (2, 5), from top to bottom. At the planar realization, $\operatorname{rank}(\mathrm{d}\boldsymbol{f} / \mathrm{d}\boldsymbol{p}) = 15$, and a first-order flex and a self-stress can be written for $a_1,\ a_2,\ a_3,\ b_1,\ b_2,\ b_3,\ b_4 \in \mathbb{R}$ as:

$$
\boldsymbol{p}' = \begin{bmatrix} 0 & 0 & 0 \\ 0 & 0 & 0 \\ 1 & 0 & 0 \\ 0 & 0 & 0 \\ 0 & 0 & 0 \\ 0 & 1 & 0 \\ 0 & 0 & 0 \\ 0 & 0 & 0 \\ 0 & 0 & 0 \\ 0 & 0 & 1 \\ 0 & 0 & 0 \\ 0 & 0 & 0 \\ 0 & 0 & 0 \\ -3 & 3 & 0 \\ 0 & 0 & 0 \\ 0 & 0 & 0 \\ 0 & 0 & 0 \\ -3 & 3 & 0 \end{bmatrix} \begin{pmatrix} a_1 \\ a_2 \\ a_3 \end{pmatrix}, \ \boldsymbol{\omega}^{\mathrm{s}} = \begin{bmatrix} 0 & 0 & 0 & 0 \\ 0 & 0 & 0 & 0 \\ 6 & 4 & 5 & -1 \\ 3 & 0 & 2 & 0 \\ 0 & 0 & 0 & 0 \\ 3 & 0 & 1 & 1 \\ 3 & 2 & 1 & -1 \\ 0 & 0 & 0 & 0 \\ 3 & 2 & 2 & -2 \\ -3 & 0 & -1 & 0 \\ -3 & 0 & -1 & 0 \\ -1 & 0 & -\frac{1}{3} & \frac{1}{3} \\ -3 & -1 & -1 & 1 \\ -3 & -1 & -1 & 1 \\ -1 & 0 & 0 & 0 \\ 0 & -1 & -1 & 1 \\ 0 & -1 & 0 & 0 \\ 0 & 0 & -1 & 0 \\ 0 & 0 & 0 & -1 \end{bmatrix} \begin{pmatrix} b_1 \\ b_2 \\ b_3 \\ b_4 \end{pmatrix}.
$$

where the columns of coefficient matrices of $(a_1,\, a_2,\, a_3)^{\mathsf{T}}$ and $(b_1,\, b_2,\, b_3,\, b_4)^{\mathsf{T}}$ are the bases of the first-order flex and the self-stress. The self-stresses corresponding to the coplanar constraints are always zero in the planar realization. At the unloaded planar realization, the matrices $\bar{\boldsymbol{P}}'^{\mathsf{T}}[\bar{\boldsymbol{\omega}}_i^{\mathrm{s}} \cdot \mathrm{d}^2\boldsymbol{f} \,/\, \mathrm{d}\boldsymbol{p}^2]\bar{\boldsymbol{P}}'$ $(i = 1,\, 2,\, 3,\, 4)$ in Eq. (55) are:

$$\bar{\boldsymbol{P}}'^{\mathsf{T}} \left[\bar{\boldsymbol{\omega}}_1^{\mathrm{s}} \cdot \frac{\mathrm{d}^2\boldsymbol{f}}{\mathrm{d}\boldsymbol{p}^2}\right] \bar{\boldsymbol{P}}' = 6 \begin{bmatrix} -1 & 5 & 0 \\ 5 & -7 & 0 \\ 0 & 0 & -1 \end{bmatrix}, \quad \bar{\boldsymbol{P}}'^{\mathsf{T}} \left[\bar{\boldsymbol{\omega}}_2^{\mathrm{s}} \cdot \frac{\mathrm{d}^2\boldsymbol{f}}{\mathrm{d}\boldsymbol{p}^2}\right] \bar{\boldsymbol{P}}' = 2 \begin{bmatrix} -5 & 7 & 0 \\ 7 & -8 & 0 \\ 0 & 0 & 0 \end{bmatrix},$$
$$\bar{\boldsymbol{P}}'^{\mathsf{T}} \left[\bar{\boldsymbol{\omega}}_3^{\mathrm{s}} \cdot \frac{\mathrm{d}^2\boldsymbol{f}}{\mathrm{d}\boldsymbol{p}^2}\right] \bar{\boldsymbol{P}}' = 2 \begin{bmatrix} -1 & 5 & 0 \\ 5 & -7 & 0 \\ 0 & 0 & -1 \end{bmatrix}, \quad \bar{\boldsymbol{P}}'^{\mathsf{T}} \left[\bar{\boldsymbol{\omega}}_4^{\mathrm{s}} \cdot \frac{\mathrm{d}^2\boldsymbol{f}}{\mathrm{d}\boldsymbol{p}^2}\right] \bar{\boldsymbol{P}}' = -2 \begin{bmatrix} -5 & 7 & 0 \\ 7 & -8 & 0 \\ 0 & 0 & 0 \end{bmatrix}.$$

On the other hand, at the three-dimensional realization, $\operatorname{rank}(\mathrm{d}\boldsymbol{f} \,/\, \mathrm{d}\boldsymbol{p}) = 16$, and a first-order flex and a self-stress can be written for $a_1,\ a_2,\ b_1,\ b_2,\ b_3 \in$

$\mathbb{R}$ as:

$$\boldsymbol{p}' = \begin{bmatrix} 1 & 0 \\ 0 & 0 \\ -1 & 0 \\ 1 & 0 \\ 0 & 0 \\ -2 & 0 \\ 0 & 0 \\ 0 & 1 \\ 0 & 0 \\ 0 & -1 \\ 0 & 0 \\ 0 & 0 \\ 0 & 0 \\ -3 & 0 \\ 3 & 0 \\ 0 & 0 \\ 0 & 0 \\ -3 & 0 \end{bmatrix} \begin{pmatrix} a_1 \\ a_2 \end{pmatrix}, \ \boldsymbol{\omega}^{\mathrm{s}} = \begin{bmatrix} 0 & \frac{1}{2} & -\frac{1}{2} \\ 0 & \frac{1}{2} & -\frac{1}{2} \\ 3 & 3 & 0 \\ 1 & -\frac{1}{2} & \frac{1}{2} \\ 0 & 0 & 0 \\ 0 & -\frac{1}{2} & \frac{3}{2} \\ 0 & \frac{3}{2} & -\frac{1}{2} \\ 0 & 0 & 0 \\ 1 & \frac{3}{2} & -\frac{3}{2} \\ 0 & 1 & -1 \\ 0 & 1 & -1 \\ 0 & \frac{1}{6} & \frac{1}{6} \\ 0 & -1 & 1 \\ 0 & -1 & 1 \\ \frac{1}{3} & \frac{1}{6} & -\frac{1}{6} \\ -1 & -1 & 1 \\ -1 & 0 & 0 \\ 0 & -1 & 0 \\ 0 & 0 & -1 \end{bmatrix} \begin{pmatrix} b_1 \\ b_2 \\ b_3 \end{pmatrix}.$$

At the unloaded three-dimensional realization, the matrices $\bar{\boldsymbol{P}}'^{\mathsf{T}}[\bar{\boldsymbol{\omega}}_i^{\mathrm{s}} \cdot \mathrm{d}^2 \boldsymbol{f} \,/\, \mathrm{d}\boldsymbol{p}^2] \bar{\boldsymbol{P}}'$

($i = 1,\, 2,\, 3$) in Eq. (55) are:

$$\bar{\boldsymbol{P}}'^{\mathsf{T}} \left[\bar{\boldsymbol{\omega}}_1^{\mathrm{s}} \cdot \frac{\mathrm{d}^2 \boldsymbol{f}}{\mathrm{d}\boldsymbol{p}^2} \right] \bar{\boldsymbol{P}}' = \boldsymbol{O}, \quad \bar{\boldsymbol{P}}'^{\mathsf{T}} \left[\bar{\boldsymbol{\omega}}_2^{\mathrm{s}} \cdot \frac{\mathrm{d}^2 \boldsymbol{f}}{\mathrm{d}\boldsymbol{p}^2} \right] \bar{\boldsymbol{P}}' = 36 \begin{bmatrix} -1 & 0 \\ 0 & 1 \end{bmatrix},$$

$$\bar{\boldsymbol{P}}'^{\mathsf{T}} \left[\bar{\boldsymbol{\omega}}_3^{\mathrm{s}} \cdot \frac{\mathrm{d}^2 \boldsymbol{f}}{\mathrm{d}\boldsymbol{p}^2} \right] \bar{\boldsymbol{P}}' = 4 \begin{bmatrix} 1 & 0 \\ 0 & -1 \end{bmatrix}.$$

When the extra boundary condition is assigned so that the z coordinate of vertex 1 is fixed, the size of the rigidity matrix is reduced to 19×17, and $\operatorname{rank}(\mathrm{d}\boldsymbol{f} \,/\, \mathrm{d}\boldsymbol{p}) = 16$. A first-order flex and a self-stress can be written for

$a,\ b_1,\ b_2,\ b_3 \in \mathbb{R}$ as:

$$\boldsymbol{p}' = \begin{pmatrix} 0 \\ 0 \\ 0 \\ 0 \\ 0 \\ 0 \\ a \\ 0 \\ -a \\ 0 \\ 0 \\ 0 \\ 0 \\ 0 \\ 0 \\ 0 \\ 0 \end{pmatrix}, \ \boldsymbol{\omega}^{\mathrm{s}} = \begin{bmatrix} 0 & \frac{1}{2} & -\frac{1}{2} \\ 0 & \frac{1}{2} & -\frac{1}{2} \\ 3 & 3 & 0 \\ 1 & -\frac{1}{2} & \frac{1}{2} \\ 0 & 0 & 0 \\ 0 & -\frac{1}{2} & \frac{3}{2} \\ 0 & \frac{3}{2} & -\frac{1}{2} \\ 0 & 0 & 0 \\ 1 & \frac{3}{2} & -\frac{3}{2} \\ 0 & 1 & -1 \\ 0 & 1 & -1 \\ 0 & \frac{1}{6} & \frac{1}{6} \\ 0 & -1 & 1 \\ 0 & -1 & 1 \\ \frac{1}{3} & \frac{1}{6} & -\frac{1}{6} \\ -1 & -1 & 1 \\ -1 & 0 & 0 \\ 0 & -1 & 0 \\ 0 & 0 & -1 \end{bmatrix} \begin{pmatrix} b_1 \\ b_2 \\ b_3 \end{pmatrix}.$$

This self-stress is the same as that of the three-dimensional realization before adding the extra boundary condition.

Appendix B. Major notation

Table B.3: Table of major notation

Rigid origami	
G	an underlying hypergraph of a rigid origami
p_i	the position vector of vertex i in $\mathbb{R}^3$
$\boldsymbol{p} = (p_1;\, p_2;\, \dots\, ;\, p_{n^{\mathrm{v}}})$	the $3n^{\mathrm{v}}$ column vector of the assemblage of $\boldsymbol{p}_i$ for all vertices
$\boldsymbol{f}^{\mathrm{c}}$	the n^{c} column vector representing the elementary coplanar constraints
$\boldsymbol{f}^{\mathrm{l}}$	the n^{l} column vector representing the elementary length constraints
$\boldsymbol{f}^{\mathrm{ca}}$	the n^{ca} column vector representing the additional coplanar constraints
$\boldsymbol{f}^{\mathrm{la}}$	the n^{la} column vector representing the additional length constraints
$\boldsymbol{f} = (\boldsymbol{f}^{\mathrm{c}};\, \boldsymbol{f}^{\mathrm{l}};\, \boldsymbol{f}^{\mathrm{ca}};\, \boldsymbol{f}^{\mathrm{la}})$	the $n^{\mathrm{c}} + n^{\mathrm{l}} + n^{\mathrm{ca}} + n^{\mathrm{la}}$ column vector of the assemblage of $\boldsymbol{f}^{\mathrm{c}}$, $\boldsymbol{f}^{\mathrm{l}}$, $\boldsymbol{f}^{\mathrm{ca}}$, and $\boldsymbol{f}^{\mathrm{la}}$
$\boldsymbol{f}^{\mathrm{b}}$	the n^{b} column vector representing the displacement boundary conditions
d_{ij}	distance between vertex i and j

$\mathcal{P}$	the solution set of $\boldsymbol{p}$ under the coplanar constraints and the fully braced length constraints for fixed d_{ij}
$O(\boldsymbol{p})$	a neighbourhood at $\boldsymbol{p}$ in the solution space $\mathcal{P}$
$\boldsymbol{p}'$	a first-order flex
$\bar{\boldsymbol{p}}'_1$, $\bar{\boldsymbol{p}}'_2$, $\ldots$, $\bar{\boldsymbol{p}}'_{n^{\mathrm{f}}}$	bases of the space of first-order flex
$\boldsymbol{\omega}^{\mathrm{c}}$, $\boldsymbol{\omega}^{\mathrm{sc}}$	the n^{c} column vectors representing an internal force and a self-stress associated with the elementary coplanar constraint $\boldsymbol{f}^{\mathrm{c}}$
$\boldsymbol{\omega}^{\mathrm{l}}$, $\boldsymbol{\omega}^{\mathrm{sl}}$	the n^{l} column vectors representing an internal force and a self-stress associated with the elementary length constraint $\boldsymbol{f}^{\mathrm{l}}$
$\boldsymbol{\omega}^{\mathrm{ca}}$, $\boldsymbol{\omega}^{\mathrm{sca}}$	the n^{ca} column vectors representing an internal force and a self-stress associated with the additional coplanar constraint $\boldsymbol{f}^{\mathrm{ca}}$
$\boldsymbol{\omega}^{\mathrm{la}}$, $\boldsymbol{\omega}^{\mathrm{sla}}$	the n^{la} column vectors representing an internal force and a self-stress associated with the additional length constraint $\boldsymbol{f}^{\mathrm{la}}$
$\boldsymbol{\omega} = (\boldsymbol{\omega}^{\mathrm{c}}; \boldsymbol{\omega}^{\mathrm{l}}; \boldsymbol{\omega}^{\mathrm{ca}}; \boldsymbol{\omega}^{\mathrm{la}})$	the $n^{\mathrm{c}}+n^{\mathrm{l}}+n^{\mathrm{ca}}+n^{\mathrm{la}}$ column vector of the assemblage of $\boldsymbol{\omega}^{\mathrm{c}}$, $\boldsymbol{\omega}^{\mathrm{l}}$, $\boldsymbol{\omega}^{\mathrm{ca}}$, and $\boldsymbol{\omega}^{\mathrm{la}}$
$\boldsymbol{\omega}^{\mathrm{s}} = (\boldsymbol{\omega}^{\mathrm{sc}}; \boldsymbol{\omega}^{\mathrm{sl}}; \boldsymbol{\omega}^{\mathrm{sca}}; \boldsymbol{\omega}^{\mathrm{sla}})$	the $n^{\mathrm{c}}+n^{\mathrm{l}}+n^{\mathrm{ca}}+n^{\mathrm{la}}$ column vector of the assemblage of $\boldsymbol{\omega}^{\mathrm{sc}}$, $\boldsymbol{\omega}^{\mathrm{sl}}$, $\boldsymbol{\omega}^{\mathrm{sca}}$, and $\boldsymbol{\omega}^{\mathrm{sla}}$
$\bar{\boldsymbol{\omega}}^{\mathrm{s}}_1$, $\bar{\boldsymbol{\omega}}^{\mathrm{s}}_2$, $\ldots$, $\bar{\boldsymbol{\omega}}^{\mathrm{s}}_{n^{\mathrm{s}}}$	bases of the space of self-stress

U	a general strain energy of a rigid origami
V	a general potential which a rigid origami is subject to
$\boldsymbol{e}$	an internal deformation corresponding to the constraints $\boldsymbol{f}$
$\boldsymbol{l}$	a load work-conjugate to a first-order flex $\boldsymbol{p}'$
$\delta\boldsymbol{p}$	a perturbation of position of vertices
Parameters	
$i,\ j,\ k,\ l$	flexible positive integers within a certain range
$m,\ n,\ q$	fixed positive integers in a statement
$a_1, a_2, \ldots, a_n$	n real parameters ($n \in \mathbb{Z}^+$)
$b_1, b_2, \ldots, b_n$	n real parameters ($n \in \mathbb{Z}^+$)
$c_1, c_2, \ldots, c_n$	n real parameters ($n \in \mathbb{Z}^+$)
$\varepsilon,\ \delta$	real numbers in all forms of $\varepsilon - \delta$ expressions
n^{v}	number of vertices of a rigid origami
n^{c}	number of elementary coplanar conditions for an entire rigid origami
n^{l}	number of elementary length constraints for an entire rigid origami
n^{ca}	number of additional coplanar constraints for an entire rigid origami
n^{la}	number of additional length constraints for an entire rigid origami

n^{f}	dimension of the space of non-trivial first-order flex of a rigid origami
n^{s}	dimension of the space of self-stress of a rigid origami
n^{b}	number of displacement boundary conditions

References

[1] Z. He, S. D. Guest, On rigid origami III: local rigidity analysis, Proceedings of the Royal Society A: Mathematical, Physical and Engineering Sciences 478 (2258) (2022) 20210589. doi:10.1098/rspa.2021.0589.

[2] E. D. Demaine, J. O'Rourke, Geometric folding algorithms: linkages, origami, polyhedra, Cambridge University Press, 2007.

[3] T. Ida, An Introduction to Computational Origami, Springer, Gewerbestrasse, Switzerland, 2020.

[4] T. Tachi, Introduction to structural origami, Journal of the International Association for Shell and Spatial Structures 60 (1) (2019) 7–18. doi:10.20898/j.iass.2019.199.004.

[5] M. Meloni, J. Cai, Q. Zhang, D. S. Lee, M. Li, R. Ma, T. E. Parashkevov, J. Feng, Engineering origami: A comprehensive review of recent applications, design methods, and tools, Advanced Science 8 (2021) 2000636. doi:10.1002/advs.202000636.

[6] T. Tachi, Simulation of rigid origami, in: R. J. Lang (Ed.), Proceedings of the 4th International Meeting of Origami Science, Mathematics, and Education (Origami4), AK Peters, 2009, pp. 175–187.

[7] M. Schenk, S. D. Guest, Origami folding: A structural engineering approach, in: P. Wang-Iverson, R. J. Lang, M. Yim (Eds.), Proceedings of the 5th International Meeting of Origami Science, Mathematics, and Education (Origami5), CRC Press, 2011, pp. 291–303.

[8] T. Zhang, K. Kawaguchi, M. Wu, A folding analysis method for origami based on the frame with kinematic indeterminacy, International Journal of Mechanical Sciences 146-147 (2018) 234–248. doi:10.1016/j.ijmecsci.2018.07.036.

[9] K. Hayakawa, M. Ohsaki, Form generation of rigid origami for approximation of a curved surface based on mechanical property of partially rigid frames, International Journal of Solids and Structures 216 (2021) 182–199. doi:10.1016/j.ijsolstr.2020.12.007.

[10] K. Hayakawa, M. Ohsaki, Equilibrium path and stability analysis of rigid origami using energy minimization of frame model, Frontiers in Built Environment 8 (Aug. 2022). doi:10.3389/fbuil.2022.995710.

[11] R. Connelly, W. Whiteley, Second-order rigidity and prestress stability for tensegrity frameworks, SIAM Journal on Discrete Mathematics 9 (3) (1996) 453–491. doi:10.1137/S0895480192229236.

[12] B. Schulze, W. Whiteley, Rigidity and scene analysis, in: J. E. Goodman, J. O'Rourke, C. D. Tóth (Eds.), Handbook of Discrete and Computational Geometry, CRC Press, 2017, pp. 1592–1632.

[13] R. Connelly, S. D. Guest, Frameworks, Tensegrities, and Symmetry, Cambridge University Press, 2022. doi:10.1017/9780511843297.

[14] J. C. Maxwell, Xlv. on reciprocal figures and diagrams of forces, The London, Edinburgh, and Dublin Philosophical Magazine and Journal of Science 27 (182) (1864) 250–261. doi:10.1080/14786446408643663.

[15] G. D. Laman, On graphs and rigidity of plane skeletal structures, Journal of Engineering Mathematics 4 (1970) 331–340. doi:10.1007/BF01534980.

[16] Y. Zhu, M. Schenk, E. T. Filipov, A review on origami simulations: from kinematics, to mechanics, toward multiphysics, Applied Mechanics Reviews 74 (3) (2022) 030801. doi:10.1115/1.4055031.

[17] T. Tachi, Design of infinitesimally and finitely flexible origami based on reciprocal figures, Journal for Geometry and Graphics 16 (2) (2012) 223–234.

[18] E. D. Demaine, M. D. Demaine, D. A. Huffman, T. C. Hull, D. Koschitz, T. Tachi, Zero-area reciprocal diagram of origami, in: Proceedings of the IASS Annual Symposium 2016, Tokyo, Japan, 2016.

[19] E. T. Filipov, K. Liu, T. Tachi, M. Schenk, G. H. Paulino, Bar and hinge models for scalable analysis of origami, International Journal of Solids and Structures 124 (2017) 26–45. doi:10.1016/j.ijsolstr.2017.05.028.

[20] K. Liu, G. H. Paulino, Nonlinear mechanics of non-rigid origami: an efficient computational approach, Proceedings of the Royal Society A: Mathematical, Physical and Engineering Sciences 473 (2206) (2017) 20170348. doi:10.1098/rspa.2017.0348.

[21] E. T. Filipov, T. Tachi, G. H. Paulino, Origami tubes assembled into stiff, yet reconfigurable structures and metamaterials, Proceedings of the National Academy of Sciences 112 (40) (2015) 12321–12326. doi:10.1073/pnas.1509465112.

[22] G. Salerno, How to recognize the order of infinitesimal mechanisms: A numerical approach, International Journal for Numerical Methods in Engineering 35 (1992) 1351–1395. doi:10.1002/nme.1620350702.

[23] R. Connelly, H. Servatius, Higher-order rigidity–What is the proper definition?, Discrete Computational Geometry 11 (1994) 193–200. doi:10.1007/BF02574003.

[24] H.-J. Schek, The force density method for form finding and computation of general networks, Computer Methods in Applied Mechanics and Engineering 3 (1) (1974) 115–134. doi:10.1016/0045-7825(74)90045-0.